

**PETROLEUM SOURCE ROCK LOGGING**

by

**J.D. Mendelson**

A.B., Brandeis University  
(1981)

SUBMITTED TO THE DEPARTMENT OF EARTH, ATMOSPHERIC, AND  
PLANETARY SCIENCES IN PARTIAL FULFILLMENT OF THE  
REQUIREMENTS FOR THE DEGREE OF

MASTER OF SCIENCE

in

Earth and Planetary Science

at the

MASSACHUSETTS INSTITUTE OF TECHNOLOGY

February, 1985

© Massachusetts Institute of Technology 1985

Signature of Author .....

Department of Earth, Atmospheric, and Planetary Sciences  
February 8, 1985

Certified by .....

.....  
M. Nafi Toksoz  
Thesis Advisor

Accepted by .....

.....  
Theodore R. Madden  
Chairman  
Departmental Committee on Graduate Students

**ARCHIVES**

MASSACHUSETTS INSTITUTE  
OF TECHNOLOGY

**MAR 05 1985**

LIBRARIES

# PETROLEUM SOURCE ROCK LOGGING

by

J.D. Mendelson

Submitted to the Department of Earth, Atmospheric, and Planetary Sciences on February 8, 1985 in partial fulfillment of the requirements for the Degree of Master of Science in Earth and Planetary Science.

## ABSTRACT

Regional distributions of organic content are an important aid in developing basin evolution and hydrocarbon generation models. An approach to evaluate hydrocarbon source rocks using resistivity, sonic, density, neutron and natural gamma ray logs is developed. Organic matter, as a constituent in sedimentary rocks, has a relatively low density, slow velocity, and is high in hydrogen content. Source rocks generally have low water content, and often exhibit abnormally high concentrations of uranium. These effects combine to make an in-situ estimation of organic content plausible. Evolution of kerogen to bitumen, oil, and gas systematically affects the above properties and it is possible to obtain a qualitative assessment of the state of maturation of a known source bed.

In this thesis logs and core data from wells in two separate oil provinces are used to test the methods of predicting total organic carbon content from log data. Two approaches are followed. The first method treats the organic matter as a rock constituent and calculates the log responses as a function of organic content. Two (rock and organic matter) and three (rock matrix, water and organic matter) component models are tested. This approach suffers because of the uncertainties of the physical properties of the organic matter. For each log type (i.e. sonic, gamma, resistivity, ...) log values are correlated with the laboratory measured total organic content. Bivariate regression helps to illustrate the efficacy of the models. In the second method, multivariate equations based on linear combinations of individual correlation coefficients are obtained. The importance of combining several logs which are organic content predictors is demonstrated. These equations can be used to predict total organic carbon content using only log data, in different parts of an oil province.

Thesis Supervisor: M.N. Toksoz

Title: Professor of Geophysics

## **ACKNOWLEDGEMENTS**

Grateful acknowledgements are due the Chevron Oil Field Research Company and Fritoil plc, for providing the data used in this thesis. D.K. Baskin, A.A. Brown, A.B. Carpenter, C.H. Cheng, J.M. Gunter, D.S. Guo, R.W. Jones, F. Lebreton, R.C.A. Peveraro, and R.H. Wilkens each provided many hours of valuable discussion. I am deeply grateful to each of them. K.A. Worrall paid careful attention to the preparation of the manuscript. A special mention is due Prof. M. Nafi Toksöz. His encouragement and guidance made this work a success.

This research was supported by the Full Waveform Acoustic Logging Consortium of the Earth Resources Laboratory, Department of Earth, Atmospheric, and Planetary Sciences, MIT.

## TABLE OF CONTENTS

ABSTRACT .....	1
ACKNOWLEDGEMENTS .....	2
1. INTRODUCTION .....	5
2. FORMATION EVALUATION OF SOURCE ROCKS .....	8
2.1 Geologic and Geochemical Conditions .....	8
2.2 Borehole Geophysical Logs .....	11
3. EXAMPLE DATA: BRITISH NORTH SEA .....	18
3.1 Background .....	18
3.2 Bivariate Analysis .....	19
3.3 Multivariate Regression Analysis and Prediction .....	25
4. EXAMPLE DATA: CALIFORNIA .....	29
4.1 Background .....	29
4.2 Bivariate Analysis .....	31
4.3 Multivariate Regression Analysis and Prediction .....	35
5. CONCLUSIONS .....	37
REFERENCES .....	40
APPENDIX A .....	44
APPENDIX B .....	49
APPENDIX C .....	50
APPENDIX D .....	51
APPENDIX E .....	52

APPENDIX F .....	53
APPENDIX G .....	55
APPENDIX H .....	57
TABLES .....	60
FIGURES .....	71

## 1. INTRODUCTION

In our understanding of petroleum genesis, hydrocarbons are generated from kerogen in sedimentary rocks through a complex process involving temperature, pressure, and time. Kerogen, solid organic matter insoluble in common organic solvents, ultimately determines the nature of hydrocarbon products which may be formed in such a source rock. For this reason, measurement of the quality and quantity of sedimentary organic matter are useful in understanding paleoenvironment and basin evolution problems.

Source rock analysis, generally performed on rock samples in the laboratory, has greatly enhanced success in hydrocarbon discovery. The ability to map source rock parameters has in the past depended on the availability of suitable rock samples. Drill cutting samples were primarily used for economic reasons, and analysis in the laboratory was often too infrequent. A method which allows quantitative analysis of source rocks in situ, such as by geophysical logging, is clearly desirable. Such a method would allow determination of source rock variables as a continuous function of depth in any borehole with a requisite suite of logs.

The downhole analysis of source rock formations is a relatively new endeavor. Many investigators have made use of an empirical correlation between radioactivity from uranium and total organic content (Leventhal et. al., 1983; Lebreton et. al., 1981; Fertl and Reike, 1979). However, this work generally suffers because uranium to organic matter ratios were found not to be constant (Calvert, 1976.) The relationship between organic content and density logs was studied by Schmoker (1979) and Smith et. al. (1968). It was

found that there should exist an inverse linear relationship between density and organic content, and this result was further supported by real data. However, for this result to be useful quantitatively, an accurate knowledge of the rock matrix and porosity was necessary. Meyer and Nederlof (1984) describe an approach using discriminant analysis to differentiate barren and organic-rich facies based on sonic, density, and resistivity logs. Unfortunately, this method does not provide any quantitative information about the organic content in absolute terms.

The present study has three main objectives:

1. Supply a *physical model* which accounts for the observed responses of the logging tools in the source rock environment.
2. *Recognize* a lithology which has high source rock potential, according to log responses.
3. Determine if any *quantitative relationships* exist between the various log responses and the geochemical source rock potential measurements from rock samples (e.g. total organic carbon content, maturation state...)

The current study is conveniently divided into three parts. Section 2 of the thesis considers the geological and geochemical factors which may control measured physical properties. Log responses are calculated based on formation properties and organic matter contents. For density, sonic, and neutron logs, volumetric average mixing laws are employed to develop the log response equations. Section 3.1 examines real data from four boreholes in the British North Sea. Bivariate regression analysis facilitates the comparison of

the actual data with the predicted responses developed in Section 2. This technique allows one to examine the behavior of each log studied in a variety of similar, but not identical, settings. Section 3.2 poses the question, "What is the best linear combination of log variables which yields the total organic content?" The solution technique used is multivariate linear least squares regression. Standardized multivariate regression equations permit one to assess the importance of each log in the combined analysis. Similarities and differences in the multivariate equations demonstrate the strengths and weaknesses inherent in using these equations as predictors. The methodology of Section 4 parallels that of Section 3, for a single well in California. Section 5 is devoted to discussion and conclusions on the merits and difficulties of this method of source rock assessment.



## 2. FORMATION EVALUATION OF SOURCE ROCKS

### 2.1 GEOLOGIC AND GEOCHEMICAL CONDITIONS

A very large fraction of the world's most prolific known source rocks are black marine shales (Degens et. al., 1981). They are differentiated from otherwise similar rocks by their relatively high organic contents. They are generally deposited in relatively quiet shallow seas or on continental margins. Preservation of the organic material is favored by reducing conditions where it cannot be oxidized biochemically.

Kerogen is the insoluble organic matter in sedimentary rocks. It is predominantly composed of hydrogen, carbon, and oxygen, and will also contain varying amounts sulfur, nitrogen, and trace elements. The nature and overall abundance of the kerogen are controlled by many factors in the depositional environment. In turn these factors dictate the type and amount of hydrocarbons which may evolve. Pressure, time, and temperature combine during the maturation process to form oil and gas by cracking the larger kerogen polymers. An effective expulsion mechanism is also necessary if the source is to be of economic interest. Thus the hydrocarbons which may be generated by a given time can be related to the product of four factors.

$$\text{Hydrocarbons Generated} = Q_1 Q_2 M(t) E,$$

where  $Q_1$  is the organic content fraction,  $Q_2$  is the organic matter quality;  $M$  is a maturity indicator, and  $E$  is the expulsion efficiency (Waples, 1982). Note that only  $M$  is a function of time. Each of these four factors is independent. There exist geochemical analyses in the laboratory for the evaluation of organic content type, quantity, and maturity. Expulsion efficiency is not well

understood and is difficult to measure quantitatively.

The fractional quantity of organic matter in a source rock is usually measured by the total organic carbon (TOC), in weight percent. The TOC can be related by a stoichiometric constant to the kerogen fraction, by assuming kerogen to have a representative formula such as  $C_{31}H_{45}O_3NS_2$  (Smith, 1969). Bitumens, heavy hydrocarbons which are cracked from the larger kerogen molecules, oil, and gas are generally the chief sources of organic carbon in the source bed. Typically oil and gas will migrate out of the source rock so the TOC reflects only kerogen plus bitumen. The bitumen free organic carbon, BFOC, reflects only the amount of kerogen present in the rock. TOC is directly measurable on samples by a variety of techniques including controlled pyrolysis, ashing, and wet chemical oxidation. Most "good" source rocks have TOC's of at least 2-4 wt. %, though 1% is average in the Gulf Coast.

Kerogen quality is a function of the type of organic material incorporated into the sediments. It has a large influence on the type and relative amounts of hydrocarbons which may be generated. The relationships among kerogen types are similar to those of the major coal groups. Following the classification of Tissot and Welte (1978), Type I kerogen is a relative of the alginites, Type III of the vitrinites, and Type II occupies an intermediate position, as does exinite. The Tissot diagram, the equivalent of the Van Krevelen diagram for coals, depicts these relationships in terms of elemental composition, as shown in Figure 1.

Type I kerogen, which has the greatest potential for oil generation, with convertability sometimes up to 80%, is the least commonly found. It is often

associated with lacustrine environments of deposition. The Green River Oil Shales are an example of such a deposit. Type II kerogens are by far the most widespread. They are associated with marine reducing environments, and are generally prone to generate oil and wet gas. Type III kerogen, sometimes referred to as "woody" kerogen, is rather more prone to generate gas than oil. Though deposited in aquatic conditions, it is made up chiefly of the remains of higher land plants and humic materials. The Manville Shales of Alberta are an example. Measurement of oxygen and hydrogen content allow evaluation of kerogen type by use of the Tissot diagram, but these measurements are difficult to make. More often oxygen and hydrogen are calculated from the amounts of water and carbon-dioxide released during pyrolysis. Microscopic examination of kerogen structure may also aid in determining type.

Maturity of the sediment is a strong function of time and temperature, and depends less strongly on the overburden pressure. The difference between hydrocarbons generated and the total hydrocarbon capacity is reflected in the effect of maturity. As temperature increases over time, kerogen cracks to form first bitumen, then oil and gas. The general maturation scheme is shown qualitatively in the Van Krevelen diagram. A variety of indirect methods exist for the laboratory determination of the maturation state. Their equivalence must often be evaluated regionally. Relative abundance of bitumen, vitrinite reflectance, spore color, and hydrogen content of the kerogen are all widely used methods. Figure 2 presents a summary of some common maturity indicators.

## **2.2 BOREHOLE GEOPHYSICAL LOGS**

This study focuses on the determination of TOC by well logging. The quantitative analysis of source rocks through well logs is more recent than its geochemical counterpart. Earlier work on the measurement of organic content using the sonic, density and neutron logs is discussed in Habinger (1983) and Hashmy (1982). An excellent overview of the relationship between organic content and natural radioactivity is found in Leventhal (1977) or Russell (1945). The use of resistivity measurements in source rock evaluation is summarized by Meissner (1984).

The organic content of a formation has varying effects on gamma ray, resistivity, density, neutron, and sonic logs. In evaluating these effects we can consider the formation surrounding the borehole to be made of three components: solid rock matrix, organic matter, and pore fluid. In some cases volumetric average models can be used to calculate the log response as a function of organic content. Relationships between natural radioactivity and TOC may be inferred from spectral gamma ray measurements, now available in the borehole as well as the laboratory. Strong evidence exists that abundances of uranium and organic carbon may be linearly related (Adams and Weaver, 1958).

### **2.2.1 Density Log**

Commercial density logs using the gamma-gamma method are sensitive to electron density. Gamma ray count rates are converted to an apparent bulk density by assuming an average atomic number - atomic weight ratio of 0.55.

The apparent bulk density may differ from the true bulk density if hydrogen (Z/A=1) concentration is high, but this effect is usually small. Volumetric averaging states that the true bulk density may be broken down into a sum of component densities, each of which is weighted by its fractional volume ( $V_i$ ) in the sample. This type of model is useful for a variety of response variables. For a sedimentary rock with  $n$  distinguishable components this implies

$$\rho_{\text{bulk}} = \sum V_i \rho_i \quad (1)$$

where

$$\sum V_i = 1 \quad (2)$$

Considering a two component system of rock matrix and organic matter, it is easy to show that a 10% increase in organic content, by volume, ought to cause a density decrease of 0.17 g/cc in true bulk density for limestone. (A commonly reported value for the density of organic matter = 1.0 g/cc is assumed throughout this work. See Kinghorn et. al. (1983) for a discussion of the effect of kerogen type on density.)

However, the results are not so simple if we want to solve equation (1) for TOC, which is measured as a *weight* percent. We consider a three-component system (formation) composed of rock matrix, organic matter, and pore fluid. Solving for TOC in terms of weight percentage yields the following relationship which is inverse linear (i.e. hyperbolic) in density:

$$TOC = a \left[ \frac{1}{\rho_k \left[ \frac{\rho_m \rho_b}{\rho_k} + \rho_m V_w - V_w - \rho_m \right]} \right] \quad (3)$$

$$1 - \frac{1}{\left[ \rho_b + \rho_m V_w - V_w - \rho_m \right]}$$

Here "a" is a constant relating TOC (% wt.) to kerogen (% wt.), usually taken as 0.7-0.8.

This equation suggests that an addition of 10% TOC by weight should in fact cause a density decrease of almost 0.50 g/cc. This function shows excellent sensitivity of bulk density to TOC. Figure 3 illustrates the effect of matrix density on the function. Replacement of part of the matrix by water-filled pores shifts these curves to the right (lower densities). Another such function, derived by Schmoker (1983) shows similar form and coefficients.

### 2.2.2 Sonic Log

The analysis of the sonic velocity log is analogous to the approach used for the density log. Volumetric averaging is again employed, here of travel times (i.e. Wyllie Transform). Again accounting for the non-linear weight-volume relationship, the same 10% increase in organic content should cause an increase in travel time of 40-50  $\mu\text{sec}/\text{ft}$ . The following equation is derived relating TOC to  $\Delta t$ . It is valid for the same three component system.

$$TOC = a \left[ \frac{1}{1 - \rho_m - \frac{\rho_m V_w - V_w - \rho_m}{\Delta t - V_w \Delta t_w + V_w \Delta t_m - \Delta t_m} (\Delta t_k - \Delta t_m)} \right] \quad (4)$$

Note the dependence on component travel times, as well as matrix density. A large source for error in this function is in the determination of the kerogen end-member travel time. A value of the kerogen travel time measured on isolated organic matter has never been reported. The approximation chosen here, 180  $\mu\text{sec}/\text{ft}$ , is the mean travel time for a "typical" coal (130  $\mu\text{sec}/\text{ft}$ ) and a "typical" oil (180  $\mu\text{sec}/\text{ft}$ ) (Schlumberger, 1984). As with density, velocity of the kerogen can also be expected to be a function of organic matter type. The effect of varying both kerogen and matrix travel times is shown in Figure 4. The function is most sensitive to a correct choice of transit times.

Unlike the effect on density, the effect of kerogen on travel time can be dependent on the shape of the inclusion (Toksöz and Cheng, 1978; Kuster and Toksöz, 1974). If organic matter is in the form of platelets (i.e. aspect ratios much smaller than unity) it could have a stronger effect on velocity than implied by the simple mixing law given in equation 4.

### 2.2.3 Neutron Porosity Log

Conventional neutron porosity logs respond to the presence of hydrogen in the formation. The technique involves bombarding the formation with neutrons of a known high energy (>3 MeV) and counting only thermal neutrons (<0.025 eV). Hydrogen is more efficient in slowing down the neutrons, by a factor of about 20, than any other element likely to be present in the formation. Interpretation is often done in terms of the hydrogen index, defined as the number of H atoms in one cubic centimeter of sample divided by the number of H atoms in one cc of water (H.I. = 1 for water). Based on measurements of hydrogen weight percent done by Issacs (1980), Carpenter (personal communication) computed an average value for H.I. = 0.67, from 37 mostly Type II kerogen samples from the Monterey Formation. If we assume, for simplicity, no H present in the matrix,

$$\Phi_{\text{meas}} = HI_{\text{water}} V_{\text{water}} + 0.67 V_{\text{ker.}} \quad (5)$$

where  $\Phi$  = porosity, HI = hydrogen index, and V = fractional volume. This is a volumetric two-component model. In this case the rock matrix is ignored and averaging is done with the hydrogen-bearing compounds pore water and kerogen. This assumption implies that bound water generally present in clay minerals will have a minor effect on the neutron log. Solving for TOC as a

function of apparent neutron porosity yields:

$$TOC = a \left[ \frac{1}{1 - \rho_m - \left( 1 - \frac{1}{\rho_m} - \frac{1}{V_w} \right) \frac{\rho_m V_w H I_k}{\Phi_N - V_w}} \right] \quad (6)$$

Here  $\Phi_N$  is the apparent neutron porosity. Any water unaccounted for will cause the calculated TOC to be too high. This holds for both sonic and density measurements as well. Figure 5 shows plots of this function for various combinations of matrix and porosity. It must be remembered that the rock matrix has been ignored in this analysis. Any hydrogen associated with the matrix, such as the water bound to hydrated clay minerals, will also cause TOC's predicted in this fashion to be too high.

#### 2.2.4 Resistivity Log

Archie (1942) showed empirically that the electrical resistivity of porous sedimentary rocks is a function of porosity, water saturation, and pore fluid resistivity:

$$R = R_w \phi^{-m} S_w^{-n} \quad (7)$$

In general,  $m$  and  $n$  usually lie close to 2. In conventional reservoir interpretation, this equation is used to calculate water and hydrocarbon saturations.

In considering resistivity log analysis in source rocks, we chose to adopt a hypothesis from Meissner (1984). In general, organic matter is deposited as part of the rock matrix. Since measured resistivity is primarily a function of the pore fluid it is likely that the presence of kerogen would have little effect on the log. Clay conductance effects, which are difficult to quantify, have been



omitted in this analysis. However, should that kerogen, over time, crack and form liquid bitumen, the resulting volume change would probably be great enough to cause water to be expelled from the source rock, and would result in decreased water saturation. It is suggested that resistivity may be a qualitative maturity indicator, but is probably not a good TOC indicator. Meissner (1984) presents an example from the Bakken shale (Western U.S.) to illustrate this point.

### **2.2.5 Natural Gamma Ray Log**

Data from numerous studies indicate good correlation between radioactivity from uranium and organic content, as seen in Figures 6-8 (Swanson, 1960; McKelvey and Nelson, 1949; Leventhal, 1981). Although the empirical association is good, a satisfactory physical model to explain this correlation still does not exist. From Figures 6-8 and similar results published elsewhere, we can conclude that an increase of one weight percent TOC corresponds to an increase of 1.5-5.0 ppm uranium.

With the recent advent of spectral gamma ray logging, one may hope to detect such variations in the sediment. Considerable effort was spent trying to understand this empirical relation. Several well-documented facts should be recognized. Some examples of well-known source beds exhibit no appreciable radioactivity anomaly. These examples are all lacustrine deposits (Meyer and Nederlof, 1984). However, the converse is not true; documented examples exist of lake deposits exhibiting significant uranium anomalies (Leventhal, 1981). Also notable are the results from Mann and Fyfe (1984) describing an experiment in which certain types of algae, when introduced into 2 ppm U

aqueous solution, were found to attain U concentration factors more than 1000 times normal. This suggests that the uranium-organic matter association may depend on the organic matter type. The same conclusion was reached by Leventhal after studying the results of uranium detection by fission track mapping of organic matter thin sections. The following results from the literature of uranium geochemistry are well established. U exists in nature with a crustal abundance around 1 ppm, and its concentration is known to be higher in granitic rocks. U readily exists in oxygenated waters in the  $U^{VI}$  state, but under reducing conditions it rapidly precipitates as  $U^{IV}$ . These facts suggest the following scenario, which represents neither sufficient nor necessary conditions. A source rock displaying a positive uranium anomaly might have been deposited along with the weathered byproducts of granitic rocks or some other source of uranium, and, such a bed was likely deposited under reducing conditions.

Given the many factors controlling U distribution, it is difficult to determine which, in a particular environment, will be the most important. This should preclude for some time the establishment of a general model for the response of the gamma ray log in source rock. We will, however, continue to rely on total gamma radiation as an indicator of clay content. Since most organic matter is associated with clays, total gamma radiation will certainly be a useful quantity for source rock identification.

### 3. EXAMPLE DATA - BRITISH NORTH SEA

#### 3.1 BACKGROUND

The Kimmeridge Formation is the major source rock in the North Sea. It is a transgressive marine shale of upper Jurassic age, deposited on top of a mid-Jurassic unconformity. As transgression continued, conditions became sufficient to create anoxic environments favorable to the preservation of organic matter. Aborted rifting created the horst and graben structures which at a later time may have permitted transmission of hydrocarbons along the fault planes, to mid- and lower Jurassic reservoirs. Figure 9 shows the relative positions of the four wells, labeled A,B,C and D, studied in this section.

Between 10-25 samples were taken from each well and analyzed for TOC in the laboratory. A total of 69 cutting, drill- and sidewall core samples were available. All samples were from the Kimmeridge. Log responses from the corresponding depths were read from the optical prints; these are tabulated along with the TOC values in Appendix A. Table 1 presents basic statistics of the data from each well. Appendix B gives details on the portions of the logging suites used.

Analysis of the data is divided into two parts. In Section 3.2, bivariate regression analysis highlights similarities and differences between each data set. TOC-well log crossplots from each well are considered separately. The success of the volumetric models for density, sonic, and neutron logs is also judged. In Section 3.3, least squares regression is used to calculate the linear

multivariate regression equation for each well. Standardized regression equations illustrate the importance of each variable in the multivariate equations. Prediction can be considerably improved by using sonic, density, neutron, and gamma ray log information simultaneously. Each multivariate regression is applied to every dataset, and mean differences between predicted and actual values are tabulated.

### **3.2 BIVARIATE ANALYSIS**

A medium resistivity, bulk density, neutron porosity, sonic travel time, and total gamma ray log are used for each well. This results in 20 possible correlations between the logs and TOC's. For each correlation, the bivariate regression equation is calculated; the regression and correlation coefficients are summarized in Table 2. Differences in the regression coefficients may be indicative of differences in the geologic environment, or of dependencies more complicated than expected. Considering the regression prediction relative to the volumetric model results may illuminate the causes of many observed differences. Differences in the regression offset coefficients are primarily functions of matrix properties and pore volume. Differences in the regression slope coefficients are primarily functions of the organic matter properties.

#### **3.2.1 DENSITY LOG v. TOC ANALYSIS**

For each well, a plot of TOC versus bulk density is constructed (Figures 10A-D). The calculated correlation coefficients from first order least squares regression are all significant, ranging from -0.681 (Well A) to -0.365 (Well B).

Combining the density and TOC values from all four wells, the resulting correlation coefficient is -0.372. This suggests that regional effects are important sources of variation in the data. Table 2 summarizes the regression and correlation coefficients for the four wells.

Wells A and D appear the most similar. These two datasets have the highest TOC's, and both appear low in water content. Better agreement between models and data is achieved in Wells B and C by assuming these shales are higher in water content. The higher regression slopes from these wells indicate that the organic matter density is relatively high.

Since they can be well approximated by linear functions, the volumetric average solutions are by definition worse predictors than the least squares lines. Specifically, the volumetric equations require an accurate knowledge of the matrix density and pore water content. It is difficult to extract the water content independent of the organic content because their physical properties are similar. (See Appendix C for a comparison.) Further, the organic matter density, which is almost certainly a function of kerogen type (Kinghorn and Rahman, 1983), may also be poorly known. These factors place serious constraints on the utility of these equations. However, when formation and organic matter properties are known, volumetric averaging will allow accurate prediction of TOC.

### **3.2.2 SONIC LOG v. TOC ANALYSIS**

Consideration of the sonic log yields results similar to the density log analysis. Correlation coefficients range from 0.882 (Well D) to 0.282 (Well B).

The correlation coefficient from the composite data of all four wells is 0.305, again suggesting that formation properties vary between the wells. Sonic log versus TOC crossplots are shown in Figures 11A-D. Again the volumetric average solutions are inadequate to explain the scatter of points about a line. Uncertainties in porosity and the presence of high-density, high-velocity minerals (especially in Well A) may be inferred from the plots. Both of these will significantly affect the measured travel times and their presence in the matrix must be taken into account.

Wells B and C again show an anomalous behavior. Increases in travel time per unit increase in TOC are much larger than for the other two wells. Kerogen travel times used to model these data were 300 and 330  $\mu\text{sec}/\text{ft}$  respectively, again suggesting differences in the kerogen in wells B and C. As with the density log, model input parameters must be well constrained if the volumetric equation is to be used for TOC prediction. A potentially large source of error lies in the value chosen for the pure kerogen travel time.

However, unlike the density log, another potential source of error lies in the mixing law chosen. The apparently high kerogen travel times noted above may be the manifestation of structural changes in the kerogen, perhaps as a result of thermal maturation. If such structural changes are common, a more complicated mixing law may be required.

### **3.2.3 NEUTRON POROSITY LOG v. TOC ANALYSIS**

Figures 12A-D are plots of apparent neutron porosity versus TOC. Correlation coefficients were 0.761 (Well A), 0.730 (Well C), 0.797 (Well D), and

0.373 (Well B). Additionally, as can be seen from the regression coefficients in Table 2, all of the neutron regression slopes are quite close. This suggests that the neutron log may be less sensitive to the choice of formation parameters than are the density and sonic logs. However, all of the volumetric model lines would significantly underestimate the measured neutron porosity if they were not corrected for pore water content.

Two factors limit the utility of the neutron model. Hydrogen associated with clay minerals is unaccounted for and will cause predicted TOC's to be too high. Also, the hydrogen index of kerogen is assumed constant at 0.67. A kerogen which is richer in hydrogen will cause the apparent neutron porosity to increase faster than expected. Such an effect may be seen in Figure 12-B.

In all the cases considered so far, the question arises as to why any given log-TOC correlation which is strong in one well should be weak in another. A near-unity correlation coefficient implies only that the data conform to a linear trend. If matrix properties change from sample to sample, then the dependence of TOC on that log need not remain the same. Conversely, when samples from a given well are fairly uniform (i.e., matrix parameters and pore water volumes are all similar), then that log-TOC crossplot should exhibit a linear tendency.

Evidence is shown to support this fact in Table 2. In Wells A and D, TOC's are generally well correlated with all the porosity logs, density, neutron, and sonic. However, in Well B, all three correlations are much poorer, and in Well C the results are only slightly better.

### **3.2.4 GAMMA RAY LOG v. TOC ANALYSIS**

Plots of gamma ray intensity versus TOC are shown in Figures 13A-D. Unfortunately, no spectral gamma ray data are available for these wells. Correlations with TOC are generally high: 0.530 for Well A, 0.810 for Well B, 0.728 for Well C, and 0.781 for Well D. However, the slopes of the regression lines vary by a factor of about four, from 0.029 (Well C) to 0.112 (well D). Refer to Table 2 for a summary of the bivariate regression analyses. Combining all four wells yields an overall correlation coefficient of 0.557.

That gamma ray response should be correlated with organic content in the Kimmeridge is not surprising. A source for terrigenous sediments was located nearby and reducing conditions, prevalent at the time of deposition, favor precipitation of the  $U^{VI}$  ion. Without spectral data it is impossible to draw firm conclusions on the source of this radioactivity anomaly. If uranium is the source, imperfect correlation may be the result of varying abundances of potassium and thorium. Likewise, sources of uranium other than organic matter will also diminish the observed correlation coefficients. This point will be discussed again in the next section, where spectral gamma ray data allow many interesting conclusions to be drawn.

### **3.2.5 RESISTIVITY LOG v. TOC ANALYSIS**

Following the results of Section 2, it is recalled that the measured resistivity is primarily a function of water content. If the inclusion of organic matter in the sediment does not influence the development of porosity, a high degree of correlation between resistivity and organic content should not be



expected. This result is borne out by the resistivity data for the Kimmeridge wells. Plots of resistivity versus TOC are shown in Figures 14A-D. Correlation coefficients are 0.426 for Well A, -0.196 for Well B, 0.460 for Well C, and -0.029 for Well D. The only conclusion drawn is that the mean resistivity for the four wells (12.5 ohm-m) is unusually high for a typical shale.

### 3.3 MULTIVARIATE REGRESSION ANALYSIS AND PREDICTION

The utility of multivariate least squares regression in determining TOC is now considered. Multivariate regression results may often be superior to univariate results, if two or more independent variables exist which are well correlated to the dependent variable but uncorrelated themselves. Mathematically, this is equivalent to having a correlation matrix with two or more dominant eigenvalues.

Correlation matrices for each well are listed in Tables 3A-D. A multiple regression equation is calculated based on each correlation matrix. Note that, for the reasons given above, resistivity is not allowed to enter into the multivariate regression equations. This equation is the best linear combination of log variables for predicting TOC in that well. The multiple regression equations are:

$$\text{TOC} = 0.099 \Delta t + 0.381 \Phi_N - 6.244 \rho_b + 0.059 \text{GR} + 10.71 \quad (8-A)$$

$$\text{TOC} = 0.044 \Delta t - 0.070 \Phi_N - 1.080 \rho_b + 0.093 \text{GR} - 1.349 \quad (8-B)$$

$$\text{TOC} = -0.044 \Delta t + 0.221 \Phi_N - 2.936 \rho_b + 0.035 \text{GR} - 10.708 \quad (8-C)$$

$$\text{TOC} = 0.084 \Delta t + 0.134 \Phi_N - 1.424 \rho_b + 0.040 \text{GR} - 5.765 \quad (8-D)$$

(See Appendix D for units.) Standardized regression equations are more meaningful when comparing the regression equations from different wells. Standard variables have a mean of zero and a standard deviation of one. Consequently, each standardized regression coefficient determines the weight given to that log in the multivariate equation. Standardization often eliminates effects due to outside influences such as depth. In terms of standardized

variables, the four regression equations are

$$\text{TOC} = 0.327 \Delta t + 0.931 \Phi_N - 0.180 \rho_b - 0.645 \text{GR} \quad (9-A)$$

$$\text{TOC} = 0.494 \Delta t - 0.344 \Phi_N - 0.077 \rho_b + 0.850 \text{GR} \quad (9-B)$$

$$\text{TOC} = -0.363 \Delta t + 0.452 \Phi_N + 0.172 \rho_b + 0.904 \text{GR} \quad (9-C)$$

$$\text{TOC} = 0.479 \Delta t + 0.295 \Phi_N - 0.072 \rho_b + 0.281 \text{GR} \quad (9-D)$$

Each variable in eqs. (9) should be read as a standard variable. Analysis of variance results are given for each regression in Tables 4A-D. All of the regressions are significant at the 95% acceptance level or better. Even after standardization, one finds no obvious similarities among the four regression equations. The log which is best correlated with TOC has the greatest weight in the regression equation. Subsequent ordering is determined by the remaining log-TOC correlations, as well as by the intercorrelations among the logs themselves. Thus there is no reason to expect any consistency between the signs of regression and correlation coefficients, except in the highest weighted term of each equation.

Another measure of the success of multivariate regression is seen in the relative increase of the multiple correlation increase,  $R_M$ , over the best bivariate correlation coefficient. For Well A,  $R_M = 0.852$ , is compared with the best bivariate correlation coefficient, 0.764, (TOC, sonic log). In Well B, the best bivariate correlation is 0.810 (gamma ray log), compared with 0.853 from multiple regression. Multiple regression in Well C achieves a correlation coefficient of 0.860; the best bivariate correlation is between TOC and neutron porosity (0.738). Well D improved from 0.797, also between TOC and the neutron log, to 0.959 for multiple correlation. Figures 15A-D are plots of TOC estimated

by multiple regression against the actual TOC values measured in the laboratory. Figure 15E is a plot of measured TOC against TOC's attained by regressing all wells simultaneously. The correlation coefficient is again lower, 0.637. The correlation matrix and ANOVA table for the combined data are shown in Table 5.

It is instructive to attempt to predict TOC values which were not included in the regression analysis, based only on log responses. This is a strong test of the utility of the least squares solutions, since the new data would in no way have been used to constrain the regression equation. Using the regression equation from one well, TOC values for each of the other three wells are predicted. Table 6 shows the correlation coefficients achieved between TOC values calculated in this way and the actual TOC values which are known from laboratory analysis. The diagonal elements of this table are the  $R_{ij}$ 's described above. Two observations can be drawn from a study of Table 6. Reading across the table, it is apparent that Wells A, C and D are successfully predicted by each of the other three regression equations. The implication is that organic content is the major source of variability in these two data sets. This supports the earlier conclusion that there is considerable non-uniformity with respect to formation properties in the Well B data. Reading the table column-wise, it appears that the regression equations from Wells B, C and D are also the most versatile. The equation from Well A is more limited in scope. This is the result of a strong TOC-density correlation in Well A which is not prominent in the other wells.

The above analysis indicates only that TOC's calculated by "cross-regression" are correlated to the measured values. A further condition which

must be met is that the absolute magnitudes also be similar. For each of the 12 possible cross-regressions, a mean-square difference is calculated as

$$\text{MSD} = \frac{1}{N} \cdot \sqrt{(\text{TOC} - \text{TOC}_{\text{est}})^2}. \quad (10)$$

These results are shown in Table 7 as the elements of a square matrix whose diagonal elements are the best results achievable with a linear equation. This analysis supports the earlier hypothesis that equations B, C, and D are the best predictive equations. The average mean-square difference for three cross-regressed wells is 2.90 % wt. (Well C), 3.01 % wt. (Well D), and 3.49 % wt., (Well B). Such errors may be intolerable for many applications.

## 4. EXAMPLE DATA - CALIFORNIA

### 4.1 BACKGROUND

The Monterey formation of the Western U.S. is thought by many to be both source and reservoir. It seems likely that at least a large fraction of Monterey oil was generated from source rocks in the organic rich phosphatic member. One of the more complex oil-bearing lithologies in the world, the Monterey seems a good choice to test the source rock models. Its organic richness and well known uranium abundance make the choice an especially attractive one. The lithology of the Monterey is lean brown siliceous shales and organic rich black biogenic shales, interbedded with layers of apatite and authigenic phosphatic inclusions. The depositional environment was most likely a high energy continental margin, with medium to deep water depths prevailing at the time of deposition. Subsequent tectonic activity during diagenesis probably played a role in the thermal evolution of the area, allowing the maturation of the organic rich sediments to proceed rapidly in a relatively young (Miocene) sediment.

Drill core through the phosphatic member provides a unique opportunity to sample the source facies at closely spaced (1 foot) intervals. 21 evenly spaced samples were chosen on the basis of spectral gamma ray log uranium response ( $10 < U < 70$  ppm). TOC, measured by controlled pyrolysis on every sample, ranged from 5 to 14 % wt., with a mean value of 9.8 % wt. Bitumen content was measured on every third sample by soxhlet extraction. Range was from 1 to 4 % wt., with a mean of 2.6 % wt. Calculated bitumen/TOC ratios indicate the organic matter to be of intermediate maturity. Core data was

interpolated to 6" samples and then smoothed with a three foot moving average filter. The resulting loss of information is felt to be small compared to the benefits gained in matching the spatial resolution of the logging measurements. Core data are shown graphically in Figure 16, and listed in tabular form in Appendix E. Logging measurements available are the same as those in the North Sea examples, except that spectral gamma ray estimates are available for uranium, thorium, and potassium concentrations. Log data is tabulated in Appendix F, and plotted versus depth in Figure 17. Details of the logging suite follow in Appendix G.

Data analysis methods parallel those used in the last section. Crossplots of TOC versus the log variables permit independent assessment of each log as an organic content indicator. The correlation coefficients in the California well are generally lower than those in the North Sea examples. This is felt to reflect the complex lithology and porosity relationships typical of the Monterey, as well as the effect of beds thinner than the vertical resolution of the logging tools. The latter effect causes averaging of the log responses and loss of bed definition. Cross regression of the Kimmeridge and Monterey data is attempted using sonic, density, neutron, and total gamma ray logs.

## **4.2 BIVARIATE ANALYSIS**

### **4.2.1 DENSITY LOG v. TOC ANALYSIS**

Figure 18 is the TOC-bulk density crossplot for the California well. Correlation coefficient is -0.330. Although there is no strong linear association, the data are in close proximity to the volumetric average model prediction. Further, the regression equation has coefficients similar to those of Kimmeridge Wells B and C (see Table 2 and Table 8). Most points exhibit lower densities than expected, suggesting the existence of another low density phase in the formation. The presence of water, either hydrated on the surfaces of clay minerals or as porosity, is typical of all shales. Some data also show higher densities than expected, indicating the presence of heavy minerals. This result is confirmed by x-ray fluorescence and electron microprobe analysis, which indicate appreciable amounts of phosphate and some pyrite in the rock. In fact 43% of the variance in ferric oxide abundance (measured by x-ray fluorescence on every sample) can be explained by TOC abundance (correlation coefficient = 0.658). This is interesting in light of work done by Schmoker (1983), where evidence was seen for a linear association between organic matter and pyrite content in the Devonian source rocks of the Appalachian Basin.

### **4.2.2 SONIC LOG v. TOC ANALYSIS**

The correlation coefficient of sonic travel time with TOC (0.493) is higher than that with density. A crossplot of the data (Figure 19) shows that, although the data are well distributed about the model line, there is less variability than



expected. Better agreement between model and data is achieved by decreasing the organic matter travel time to 170  $\mu\text{sec}/\text{ft}$ . The lack of fit at extreme values of travel time is also the result of the averaging of travel times in layers thinner than the source-receiver separation of the logging tool.

#### 4.2.3 NEUTRON POROSITY LOG v. TOC ANALYSIS

The case of the neutron log is anomalous (Figure 20). The calculated correlation coefficient, though not highly significant (-0.353), suggests that the apparent neutron porosity decreases as TOC increases. This situation is physically unrealizable unless bitumen generation has forced a significant expulsion of water from the rock. This should, in turn, cause a measurable increase in resistivity. However, study of the correlation matrices for TOC, bitumen, and bitumen-free organic carbon indicates that this is not the case (see Tables 9-11).

The apparently high porosity values may be explained by one or more reasons. As for the other porosity logs, water-filled porosity, insufficient tool resolution, and uncertainty in the model parameters almost certainly play a part in the failure of the models to accurately predict organic content. In addition, specific to the neutron log, overestimation of the hydrogen index could be a factor, although this is unlikely. Also, the presence of efficient neutron absorbers as trace elements (such as boron) is not unknown in the Monterey. Such factors preclude saying any more about the response of the neutron log in this instance.

#### 4.2.4 RESISTIVITY LOG v. TOC ANALYSIS

As expected, the resistivity log shows no significant correlation with TOC (correlation coefficient = -0.151). However, as a potential maturity indicator, one might expect the resistivity measurement to correlate with either bitumen content or the bitumen-TOC ratio.

Rewriting equation (7) in terms of conductivities and setting the saturation and cementation exponents = 2,

$$C = C_w(\phi S_w)^2, \quad (11)$$

it is apparent that any volumetric change in the water content should be reflected as a linear change in  $\sqrt{C}$ . Bitumen versus  $\sqrt{C}$  is plotted for the Monterey data in Figure 21. Although the correlation coefficient (-0.261) is not strong, this does support the hypothesis of Meissner (1981) that resistivity may at least make a qualitative maturity indicator.

#### 4.2.5 SPECTRAL GAMMA RAY LOG v. TOC ANALYSIS

An abundance of radioactive elements, particularly uranium, and the availability of a spectral gamma ray log make it feasible to study the relationship between uranium and organic matter. However, this relationship is complicated by the presence of the phosphatic minerals, as they are also known to have a chemical affinity for uranium (Calvert, 1981).

As seen in the summary of bivariate regressions (Table 8) and log-core crossplots (Figures 22-24), thorium has the best correlation with TOC (0.641).

Uranium was next highest (0.562), and potassium also showed association, (0.341). It is expected that thorium and potassium should also show some degree of correlation with TOC because they are generally good indicators of clay content, and clay is often associated with organic matter in source rock shales. The apparently low correlation for uranium is likely the result of two effects. The vertical resolution of the tool with respect to thin beds (see core photograph, Figure 26) is certainly inadequate to accurately reconstruct the true uranium distribution in the rock. Secondly, any uranium associated with the phosphates need not correlate with organic content.

In order to overcome these problems, the core was resampled, again at one foot intervals. The samples were crushed, ground by an agate mill, and split for three analyses. Samples were analyzed for total organic carbon by wet chemical oxidation, uranium by delayed neutron counting, and elemental composition (in terms of oxides) by x-ray fluorescence. These new data, tabulated in Appendix H, are most illuminating. Figure 25 is a three-dimensional crossplot of the new data. TOC (y-axis) is plotted against uranium abundance (x-axis);  $P_2O_5$  is shown on the z-axis in terms of color. The points which are low in phosphate and high in organic content fall nearly on a line, with uranium increasing at a rate of roughly 2.5 ppm for every TOC wt. % unit. The dependence of uranium on phosphate is more variable, but has roughly the magnitude of 1.5-3.0 ppm U per wt. %  $P_2O_5$  unit. While this is not enough to formulate a general model, it is useful for two reasons. The results of other authors have been confirmed for a new geologic environment; and it seems that uranium is a good TOC predictor in this setting, provided phosphate content is taken into account. In fact, regressing TOC and phosphate contents on uranium explains over 90% of the total uranium variability in this example ( $R_M = 0.954$ ).

#### 4.3 MULTIVARIATE REGRESSION ANALYSIS AND PREDICTION

A multivariate regression equation is calculated from the TOC correlation matrix (Table 8). Again, resistivity is excluded from the analysis. The multiple correlation coefficient (0.862) represents a significant improvement over the best bivariate correlation coefficient (0.650, for TOC and total gamma ray). The analysis of variance results in Table 12 show this equation is significant at the 99% acceptance level. When used to predict the TOC values which constrained the regression, approximately 74% percent of the original variance is recovered. Measured versus estimated TOC's are plotted in Figure 27. The calculated regression equation is

$$\begin{aligned} \text{TOC} = & -0.068 \Delta t - 0.247 \Phi_N - 7.195 \rho_b + 0.028 \text{GR} + 0.459 \text{T} \\ & + 0.080 \text{U} - 1.367 \text{K} + 26.808 \end{aligned} \quad (12)$$

For the purposes of comparison with the North Sea well data, a limited regression equation is calculated which does not make use of the thorium, uranium, or potassium data. This equation is

$$\text{TOC} = 0.095 \Delta t - 0.480 \Phi_N - 5.499 \rho_b + 0.041 \text{GR} + 18.134 \quad (13)$$

or in terms of standardized regression coefficients,

$$\text{TOC} = 0.249 \Delta t - 0.299 \Phi_N - 0.247 \rho_b + 0.665 \text{GR} \quad (14)$$

Although there are no obvious similarities to any of the North Sea regression equations, it is instructive to consider the cross-regression correlation and mean square difference tables (Tables 13 and 14).

While there are no apparent correlations between the TOC's predicted with the California limited regression equation and the actual TOC's from the North

Sea wells, the mean square difference for all North Sea TOC's is 3.19% wt. Conversely, when the Kimmeridge regression equations are used to predict the Monterey data, the average mean square difference is 4.29% wt. Only the regression equation from Kimmeridge Well D showed real success, with a mean square difference value of 1.22% wt.

## 5. DISCUSSION AND CONCLUSIONS

The preceding sections describe in detail the in-situ evaluation of source rocks as compared with conventional laboratory analysis. Comparison of log and sample data from 5 wells in two widely separated oil provinces suggest that current borehole tools may evaluate total organic carbon content. Simple physical models have been developed to explain the responses of sonic, density, and neutron logs in the source rock environment. These models show good agreement with some observations from real data. Uranium content also shows a high degree of correlation with organic carbon in the Monterey formation. These facts combine to make downhole evaluation of source rock feasible.

The volumetric average models developed for sonic, density, and neutron logs in Section 2 are mixing laws which calculate log responses as a function of organic content and formation properties. Two- (rock matrix and organic matter) and three- (rock matrix, pore water, and organic matter) component models are presented. If matrix and pore fluid properties are known, TOC predictions agree quite well with real data. Sensitivities of the volumetric models to rock properties are shown in Figures 3, 4, and 5.

Bivariate regression of logs versus TOC confirms these dependencies. Differences of the regression slope and offset parameters from those of the models are indicative of the source of error in the models. Regression offsets depend strongly on rock matrix properties and pore content, while slopes are more sensitive to organic matter properties.

In studying the bivariate regression coefficients of the North Sea wells (Table 2), it becomes apparent that Well A and D data are similar, as are the data from Wells B and C. Wells A and D contain less water, and have lower matrix densities and lower matrix travel times. Additionally, there are indications that the organic matter in Wells A and D is faster and more dense. As the TOC's are also quite high, one might conclude that these rocks are less mature than their counterparts in Wells B and C. Conversely, lower TOC's in Wells B and C may be an indication that kerogen is transforming to bitumen while oil and gas are beginning to migrate out of the source rock. This is consistent with the observation of a slower, less dense organic matter phase.

It should be noted that the neutron log is more often well correlated with organic content. This is because the neutron log is less sensitive to many formation properties. However, an accurate knowledge of pore volume is quite important when using the neutron response.

In all cases log-TOC correlations are lower when the North Sea data is all grouped together. As the number of sample points increases, so do the sources of variability entering the data. Regionally varying formation properties, such as compaction, may limit global application of the regression equations.

In all the cases studied, multivariate regression, significantly improves the ability to predict TOC within each dataset. However, there are no obvious similarities among any of the multivariate equations, so there success at prediction of new data may be sporadic.

Three further problems make difficult the downhole evaluation of source rocks. The volume of sample investigated by core measurement is much smaller than that seen by the logging measurements. This makes it difficult to determine any property which varies more rapidly than the core sampling interval. Thinly laminated rocks compound this problem. The spatial resolution of the logging probe is in general limited by a characteristic physical distance or measurement path. Properties varying on a scale finer than this will be averaged into a larger investigative volume. Finally, existing data on the physical properties (density, travel time, hydrogen index) of organic matter are far too uncommon. It would seem appropriate that future research concentrate in these areas.



## REFERENCES

- Adams, J.A.S., C.E. Weaver, Thorium-to-uranium ratios as indicators of sedimentary processes: example of concept of geochemical facies, *AAPG Bull.*, 42, 387-430, 1958.
- Ayres, M.G., M. Bilal, R.W. Jones, L.W. Slentz, M. Tartir, A.O. Wilson, Hydrocarbon habitat in main producing areas, Saudi Arabia, *AAPG Bull.*, 66, 1-9, 1982.
- Calvert, S.E., N. B. Price, Geochemistry of Namibian Shelf Sediments, in *Coastal Upwelling*, Suess, E., J. Thiede, eds., Plenum Publishing Corp., New York, 1983.
- Calvert, S.E., The mineralogy and geochemistry of near-shore sediments, in *Chemical Oceanography, 2nd ed.*, Riley, J.P., R. Chester, eds., Academic Press, London, 1976.
- Degens, E.T., W. Michaelis, A. Paluska, Principles of petroleum source bed for nation, in *Energy - Present and Future Operations*, John Wiley and Sons, New York, 1981.
- Davis, J.C., *Statistics and Data Analysis in Geology*, John Wiley and Sons, New York, 1982.
- Doig, R., Natural gamma ray flux: in-situ analysis, *Geophysics*, 33, 311-328, 1968.
- Dow, W.G., Petroleum source beds on continental slopes and rises, *AAPG Bull.*, 62, 1584-1606, 1978.
- Durand, B., *Kerogen*, Technip, Paris, 1980.
- Dypvik, H., D.O. Eriksen, Natural radioactivity of clastic sediments and the contributions of U, Th, and K, *J. Petr. Geol.*, 5, 409-416, 1982.
- Fertl, W.H., W.L. Stapp, D.B. Vaello, W.C. Vercillino, Spectral gamma ray logging in the Texas Austin Chalk Trend, *SPE 7431*, 1980.
- Fertl, W.H., H.H. Reike, Gamma ray spectral evaluation techniques help identify fractured shale resevoirs and source rock characteristics, *SPE 8454*, 1979.
- Gadeken, L.L., D.M. Arnold, H.D. Smith Jr., Applications of the compensated spectral natura' gamma tool, *SPWLA Trans.*, paper JJJ, 1984.
- Gallois, R.W., A pilot study of oil shale occurrences in the Kimmeridge Clay, *Institute of Geological Sciences, National Environmental Research Council, report 78/13*, H.R.M. Stationery Office, London, 1978.
- Goff, J.C., Hydrocarbon generation and migration from Jurassic source rocks in the E. Shetland basin and Viking Graben of the northern North Sea, *J. Geol. Soc. London*, 140, 445-474, 1983.
- Hashmy, K.H., T. Hefter, R. Chicks, Quantitative log evaluation of the Devonian shales of the northeastern United States, *SPE/DOE 10795*, 1982.

- Hassan, M., A. Hossin, A. Combaz, Fundamentals of the differential gamma ray log, *SPWLA Trans.*, paper H, 1976.
- Hassan, M., The use of radioelements in diagenetical studies of shale and carbonate sediments, *Colloque International Petrographie de la Matiere Organique des sediments*, Paris, 1973.
- Hendrickson, T.A., *Synthetic Fuels Data Handbook*, Cameron Engineers, Inc., Denver, Colorado, 1975.
- Hodson, G., W.H. Fertl, G.W. Hammack, Formationsbestimmungen in Jura-sandsteinen der noerdlichen Nordsee, *Erdoel-Erdgas Zeitschrift*, 92, 151-159, 1976.
- Issacs, C., Diagenesis in the Monterey formation examined laterally along the coast near Santa Barbara, California, *Stanford University Ph.D. Thesis*, 1980.
- Johnson, R.A., D.W. Wichern, *Applied Multivariate Statistical Analysis*, Prentice Hall, Englewood Cliffs, New Jersey, 1982.
- Kinghorn, R.R.F., M. Rahman, Specific gravity as a kerogen type and maturation indicator with special reference to amorphous kerogens, *J. Petr. Geol.*, 6, 2, 179-194, 1983.
- Kuster, G.T., and M.N. Toksoz, Velocity and attenuation of seismic waves in two-phase media: part I. theoretical formulations, *Geophysics*, 39, 587-618, 1974.
- Lebreton, F., J. Dellenbach, Criteres d'analyses des roches-meres argileuses par diagraphies, *Societe pour l'Avancement d'Interpretation des Diagraphies, Inf. Letters*, Paris, May 1981.
- Leventhal, J.S., Pyrolysis gas chromatography-mass spectrometry to characterize organic matter and its relationship to uranium content of Appalachian devonian black shales, *Geochem. and Cosmochem. Acta*, 45, 883-889, 1981.
- Leventhal, J.S., Limitations of rock-eval pyrolysis assay to characterize kerogen, *AAPG Bull.*, 64, 593-598, 1982.
- Leventhal, J.S., P.H. Briggs, J.W. Baker, Geochemistry of the Chatanooga Shale, Dekalb County, central Tennessee, *Southeastern Geol.*, 24, 3, 101-116, 1983.
- Lock, G.A., W.A. Hoyer, Natural gamma ray spectral logging, *The Log Analyst*, 12, 5, 1971.
- Mann, H., W.S. Fyfe, An experimental study of algal uptake of U, Ba, V, Co, and Ni from dilute solution, *Chem. Geol.*, 44, 385-398, 1984.
- Marett, G., P. Chevalier, P. Souhatie, J. Suau, Shaly sand evaluation using gamma ray spectrometry, applied to the North Sea Jurassic, *SPWLA Trans.*, paper DD, 1976.

- McKelvey, V.E., J.M. Nelson, Characteristics of marine uranium bearing sedimentary rocks, *Econ. Geol.*, **6**, 35-53, 1945.
- Meissner, F.F., Case studies of hydrocarbon generation and migration (Williston basin, Powder River basin, and San Juan Basin), *AAPG Geochemistry for Geologists*, Dallas, Texas, 1981.
- Mendelson, J.D., The application of multivariate statistics to the detection of source rocks from well logs, *MIT paper*, 12.592, 1984.
- Meyer, B.L., M.H. Nederlof, Identification of source rocks on wireline logs by density/resistivity and sonic transit time/resistivity crossplots, *AAPG Bull.*, **68**, 121-129, 1984.
- Mo, T., A.D. Suttle, W.M. Sackett, Uranium concentration in marine sediments, *Geochem. and Cosmochem. Acta*, **37**, 1973.
- Momper, J., *Physical and Chemical Constraints on Petroleum Migration*, AAPG Continuing Education Source Note Series 8, Tulsa, 1978.
- Neumann, H.J., B. Paczynska-Lahme, D. Severin, *Composition and Properties of Petroleum*, Halsted Press, New York, 1981.
- Nriagu, J.O., P.B. Moore, *Phosphate Minerals*, Springer Verlag, Berlin, 1984.
- Russell, W.L., Relation of radioactivity, organic content, and sedimentation, *AAPG Bull.*, **29**, 1470-1494, 1945.
- Schmoker, J.W., T.C. Hester, Organic carbon in Bakken Formation, U.S. portion of Williston Basin, *AAPG Bull.*, **67**, 12, 1983.
- Schmoker, J.W., Determination of organic content of Appalachian Devonian shales from formation density logs, *AAPG Bull.*, **63**, 1504-1537, 1979.
- Schowalter, T.T., P.D. Hess, Interpretation of subsurface hydrocarbon shows, *AAPG Bull.*, **66**, 1302-1327, 1982.
- Serra, O., Theory, interpretation, and practical applications of natural gamma ray spectroscopy, *SPWLA Trans.*, paper Q, 1980.
- Simoneit, B.R.T., The organic chemistry of marine sediments, in *Chemical Oceanography*, 2nd ed., Riley, J.P., R. Chester, eds., Academic Press, London, 1976.
- Smith, J.W., Theoretical relationship between density and oil yield for oil shales, *USBM Report of Investigations 7248*, 1969.
- Swanson, V.E., Oil yield and uranium content of black shales, *USGS Prof. Paper n. 356*, 1960.
- Tissot, B.P., D.H. Welte, *Petroleum Formation and Occurrences*, Springer Verlag, Berlin, 1978.
- Tissot, B., B. Durand, J. Espitalie, A. Combaz, Influence of nature and diagenesis of organic matter in formation of petroleum, in *Hydrocarbon Generation*

*and Source Rock Evaluation, (Origin of Petroleum III)*, AAPG Reprint Series, 24, Tulsa, Oklahoma, 1982.

Toksoz, M.N., C.H. Cheng, Modeling of seismic velocities in porous rocks and its application to seismic exploration, *Arab. Jour. Sci. Eng., Special Issue*, 1978.

Waples, D.W., Phosphate-rich sedimentary rocks: significance for organic facies and petroleum exploration, *J. Geochem. Expl.*, 16, 135-160, 1982.

Waples, D.W., Simple method for oil source bed evaluation, in *Hydrocarbon Generation and Source Rock Evaluation, (Origin of Petroleum III)*, AAPG Reprint Series, 24, Tulsa, Oklahoma, 1982.

Wedepohl, K.H., Environmental influences on the chemical composition of shales and clays, in: *Physics and Chemistry of the Earth, vol. 8*, Ahrens, L.H., F. Press, S.K. Runcorn, H.C. Urey, eds., Pergamon Press, 1984.

Wichmann, P.A., V.C. McWhirter, E.C. Hopkinson, Field results of the natural gamma ray spectralog, *SPWLA Trans., paper O*, 1975.

Wiley, R., R.J. Zittel, Natural gamma ray data of various sandstones, *SPWLA Trans., paper K*, 1982.

APPENDIX A

NORTH SEA WELL DATA

**NORTH SEA WELL A**

TOC	Resistivity	Density	Neutron	Sonic	Gamma ray
9.390	17.0	2.470	27.0	80.0	110.0
6.220	18.0	2.540	24.0	75.0	100.0
12.600	14.0	2.290	30.0	88.0	120.0
1.230	10.0	2.520	9.0	66.0	86.0
7.820	12.0	2.500	20.0	102.0	80.0
1.500	9.0	2.520	12.0	72.0	70.0
1.370	14.0	2.570	12.0	67.0	78.0
3.910	3.0	2.300	18.0	83.0	70.0
1.760	13.0	2.540	11.0	70.0	80.0
1.520	14.0	2.700	10.0	66.0	60.0
1.220	17.0	2.570	7.0	65.0	60.0
7.320	14.0	2.470	20.0	80.0	108.0
2.740	21.0	2.530	18.0	70.0	116.0
3.060	16.0	2.530	25.0	73.0	116.0
4.280	23.0	2.470	29.0	84.0	125.0
3.650	23.0	2.520	27.0	81.0	140.0
3.970	20.0	2.470	27.0	78.0	137.0
6.150	13.0	2.380	30.0	92.0	180.0
4.160	19.0	2.400	28.0	88.0	144.0
4.870	35.0	2.300	33.0	97.0	190.0
3.400	45.0	2.290	38.0	101.0	165.0
2.800	23.0	2.310	37.0	102.0	190.0
3.920	19.0	2.420	25.0	70.0	140.0
6.460	18.0	2.400	32.0	95.0	170.0

**NORTH SEA WELL B**

TOC	Resistivity	Density	Neutron	Sonic	Gamma ray
5.970	4.7	2.180	41.0	125.0	60.0
4.420	4.0	2.190	47.0	127.0	65.0
4.560	4.0	2.230	43.0	127.0	57.0
0.620	7.0	2.360	27.0	93.0	44.0
2.410	5.2	2.310	34.0	110.5	44.0
2.000	6.5	2.470	29.0	103.0	30.0
2.120	5.5	2.300	37.0	110.0	45.0
2.020	5.0	2.330	37.0	105.0	47.0
1.600	10.0	2.480	24.0	100.0	33.0
1.610	5.6	2.400	33.0	103.0	43.0
1.610	7.0	2.420	32.0	97.0	38.0
1.980	7.0	2.370	35.0	103.0	44.0
1.430	13.0	2.550	24.0	73.5	32.0
2.820	6.1	2.380	31.0	94.0	65.0
1.490	8.5	2.560	18.0	73.0	43.0
3.140	7.0	2.500	25.0	79.0	62.0
2.330	7.0	2.510	25.0	80.0	57.0
3.070	18.0	2.460	22.0	73.0	53.0
3.650	6.3	2.440	22.0	75.0	48.0
4.990	7.4	2.470	30.0	86.0	77.0
6.070	8.1	2.470	28.0	90.0	82.0

NORTH SEA WELL C

TOC	Resistivity	Density	Neutron	Sonic	Gamma ray
0.95	1.5	2.70	27.0	80.0	60.0
1.41	2.0	2.47	28.0	105.0	80.0
4.35	8.0	2.38	36.0	112.0	180.0
6.40	12.0	2.30	36.0	117.0	195.0
4.83	3.3	2.42	34.0	118.0	160.0
2.75	5.0	2.40	35.0	100.0	120.0
1.08	6.0	2.45	30.0	85.0	80.0
4.43	8.0	2.42	32.0	95.0	110.0
3.11	3.0	2.40	38.0	90.0	75.0
1.92	3.5	2.47	28.0	82.0	70.0
5.37	75.0	2.60	35.0	75.0	80.0



**NORTH SEA WELL D**

TOC	Resistivity	Density	Neutron	Sonic	Gamma ray
5.23	3.5	2.44	31.0	90.0	65.0
8.26	4.5	2.47	33.0	104.0	115.0
9.01	4.5	2.46	30.0	105.0	105.0
5.92	4.0	2.55	29.0	97.0	70.0
6.36	3.5	2.55	32.0	97.0	75.0
7.86	9.5	2.42	36.0	108.0	100.0
6.24	9.0	2.47	32.0	95.0	90.0
5.41	54.0	2.44	33.0	73.0	75.0
7.24	9.0	2.20	37.0	92.0	80.0
1.83	8.0	2.75	22.0	65.0	75.0
6.04	26.0	2.42	35.0	85.0	90.0
3.63	10.0	2.46	31.0	83.0	75.0
0.70	5.0	2.57	18.0	70.0	55.0

## APPENDIX B

### NORTH SEA LOGGING SUITES

All logs were run by Schlumberger.

Resistivity	Well A Well B Well C Well D	Deep induction log Medium induction log Spherically-focused log Spherically-focused log
Density		Dual detector Formation density compensated
Neutron		Dual detector compensated Thermal neutron
Sonic		Borehole compensated 3'-5'
Gamma ray		Total gamma ray only Scintillation detector

## APPENDIX C

### RELEVANT PHYSICAL PROPERTIES OF KEROGEN AND WATER

Property	Range of Reported Values <sup>a</sup>	Value Used in Text	Source	Distilled Water Room Temperature
Density (gm/cc)	0.6-1.3	1.0	Smith (1969)	1.0
Acoustic transit time (microsec/ft)	<sup>b</sup>	180	mean value coal and oil (Schlumberger, 1984)	189
Hydrogen Index (atoms/atoms)	<sup>b</sup>	0.67	meas. H wt. % Issacs (1980)	1.00

<sup>a</sup> The actual value is a function of the kerogen type in the sample under investigation.

<sup>b</sup> No values have been reported in the literature for this property.

## APPENDIX D

### UNITS OF GEOPHYSICAL AND GEOCHEMICAL MEASUREMENTS USED IN TEXT

Mnemonic or Symbol	Measurement	Unit
R, RES	Resistivity	ohm-meter
$\Delta t$ , SON, DT	Sonic Travel Time	microsec/ft
$\rho_b$ , RHOB	Apparent Bulk Density	grams/cc
$\varphi_n$ , NPHI	Apparent Neutron Porosity Index	limestone porosity unit <sup>a</sup>
GR	Gamma Ray	API unit
U	Uranium	ppm
Th	Thorium	ppm
K	Potassium	weight percent
TOC	Total Organic Carbon	weight percent
BFOC	Bitumen-Free Organic Carbon	weight percent
BIT	Bitumen	weight percent

<sup>a</sup> Porosity units are equivalent to percent by volume. Tools are calibrated with a water-filled limestone standard.

**APPENDIX E**

**DATA FROM GEOCHEMICAL CORE ANALYSES**

**CALIFORNIA WELL**

Depth	TOC	"smooth" TOC	Bitumen	"smooth" Bitumen	BFOC	BIT/BFOC
1.0	2.32	9.05		2.74	7.00	0.39
1.5		8.05		2.73	6.01	0.45
2.0	14.00	6.82		2.38	5.04	0.47
2.5		5.66		2.04	4.14	0.49
3.0	2.17	5.71	0.65	1.69	4.45	0.38
3.5		7.42		1.34	6.41	0.21
4.0	2.67	7.45		1.00	6.71	0.15
4.5		7.75		1.13	6.91	0.16
5.0	14.25	9.74		1.61	8.53	0.19
5.5		10.72		2.09	9.15	0.23
6.0	16.08	11.62	4.01	2.57	9.69	0.27
6.5		11.54		3.05	9.25	0.33
7.0	9.00	9.81		3.53	7.16	0.49
7.5		10.88		4.03	7.86	0.51
8.0	2.12	11.70		4.05	8.66	0.47
8.5		10.47		4.06	7.42	0.55
9.0	21.78	10.25	4.13	4.08	7.19	0.57
9.5		9.34		4.10	6.27	0.65
10.0	7.47	9.42		4.12	6.33	0.65
10.5		10.34		3.77	7.51	0.50
11.0	2.65	8.44		3.40	5.89	0.58
11.5		5.71		3.04	3.43	0.89
12.0	8.54	5.03	1.58	2.67	3.02	0.89
12.5		6.78		2.31	5.05	0.46
13.0	2.67	9.22		1.95	7.76	0.25
13.5		9.96		1.63	8.74	0.19
14.0	19.71	9.87		1.67	8.61	0.19
14.5		11.02		1.72	9.73	0.18
15.0	7.89	13.01	1.90	1.76	11.69	0.15
15.5		13.36		1.81	12.01	0.15
16.0	16.59	11.28		1.85	9.89	0.19
16.5		10.70		2.00	9.20	0.22
17.0	5.16	11.81		2.11	10.23	0.21
17.5		11.83		2.21	10.17	0.22
18.0	15.65	10.61	2.64	2.32	8.86	0.26
18.5		10.44		2.43	8.62	0.28
19.0	8.02	11.91		2.53	10.01	0.25
19.5		12.64		2.91	10.48	0.28
20.0	15.44	11.88		3.17	9.50	0.33
20.5		10.71		3.44	8.13	0.42
21.0	10.28	10.64	4.50	3.70	7.86	0.47

All depths are in feet, from top of core.

**APPENDIX F**

**DATA FROM GEOPHYSICAL LOGS**

**CALIFORNIA WELLS**

Depth	Resis- tivity	Dens- ity	Neut- ron	Sonic	Gamma Ray	Thor- ium	Uran- ium	Potas- sium
1.0	19.4	2.03	28.3	94.0	171.3	5.4	40.1	1.76
1.5	17.8	2.04	27.6	91.7	149.9	6.2	39.7	1.78
2.0	16.0	2.17	27.9	88.2	137.9	6.7	37.1	1.73
2.5	16.2	2.28	28.5	85.3	143.1	6.5	33.7	1.87
3.0	19.4	2.22	28.6	86.8	151.5	6.8	31.0	1.86
3.5	22.0	2.07	28.3	90.8	152.2	6.5	33.8	1.54
4.0	19.6	2.00	28.1	94.1	136.2	6.2	36.1	1.20
4.5	15.9	2.02	27.8	99.3	125.8	8.9	34.4	1.14
5.0	18.1	2.04	27.3	102.9	127.4	11.6	30.9	1.18
5.5	20.5	2.07	26.7	100.0	140.1	14.2	28.5	1.21
6.0	21.7	2.09	26.2	94.4	158.0	13.7	33.3	1.42
6.5	19.8	2.11	26.1	93.4	183.1	11.7	42.2	1.58
7.0	16.7	2.13	26.5	96.3	196.1	9.8	44.6	1.66
7.5	14.4	2.15	26.9	98.7	192.4	9.5	42.4	1.58
8.0	13.3	2.17	26.5	98.2	179.0	9.7	41.2	1.48
8.5	12.6	2.20	25.8	95.4	172.0	10.0	41.7	1.39
9.0	12.4	2.20	25.5	92.9	186.2	10.1	42.8	1.60
9.5	13.4	2.20	25.9	90.7	204.4	8.2	50.0	1.64
10.0	15.7	2.22	26.6	89.2	207.5	6.7	54.7	1.37
10.5	17.7	2.26	27.5	89.2	189.3	6.4	51.1	1.15
11.0	19.5	2.30	28.4	88.8	162.4	6.2	44.4	1.17
11.5	21.3	2.31	28.9	89.8	150.6	6.8	38.1	1.34
12.0	23.3	2.27	28.7	93.2	150.0	6.7	33.8	1.36
12.5	22.1	2.17	27.1	96.3	149.6	7.2	32.7	1.23
13.0	18.0	2.04	25.2	99.1	145.5	8.0	33.5	1.07
13.5	13.1	1.99	25.2	101.3	145.4	9.2	34.1	0.95
14.0	12.0	2.00	25.5	102.2	153.0	10.0	33.6	1.12
14.5	14.4	2.03	25.9	101.1	168.8	11.0	36.7	1.45
15.0	17.8	2.05	26.9	99.3	189.1	11.8	44.8	1.70
15.5	18.1	2.05	27.8	99.3	205.6	12.8	51.3	1.93
16.0	15.8	2.03	28.3	102.0	215.4	13.1	53.9	1.97
16.5	15.4	2.01	28.9	103.6	220.6	11.1	54.6	2.02
17.0	18.2	2.00	29.8	104.4	221.3	10.2	53.6	2.15
17.5	20.3	2.04	29.8	103.9	213.8	10.5	52.4	2.13
18.0	21.1	2.11	27.8	102.4	207.1	11.0	50.3	2.19
18.5	20.5	2.15	25.5	100.6	211.8	11.2	49.0	2.17
19.0	20.7	2.17	24.7	98.4	223.4	10.8	52.8	1.98
19.5	21.3	2.20	25.4	95.1	235.0	9.4	58.3	1.89
20.0	21.2	2.23	26.5	90.1	242.5	7.3	62.3	2.11
20.5	19.0	2.22	27.5	87.5	244.4	5.9	64.0	2.33
21.0	17.5	2.15	28.4	86.7	242.6	5.3	63.8	2.33

All depths are in feet, from top of core.



## APPENDIX G

### CALIFORNIA WELL LOGGING SUITE

All logs were run by Dresser Atlas.

Resistivity	Shallow laterolog
Density	Dual detector Formation density compensated
Neutron	Dual detector compensated Thermal neutron
Sonic	Borehole compensated 3'-5'
Gamma ray	Scintillation detector 3 channel spectrum analyzer

## APPENDIX H

### CORE MEASUREMENTS OF URANIUM, TOC AND $P_2O_5$

Uranium content by delayed neutron counting

Organic carbon content by wet chemistry

$P_2O_5$  by x-ray fluorescence

Depth	Uranium	TOC	P <sub>2</sub> O <sub>5</sub>
1.0	5.3	2.40	3.14
2.0	28.9	8.45	9.10
3.0	3.2	1.95	0.97
4.0	3.1	2.70	1.17
6.0	32.6	10.50	8.81
7.0	12.5	7.45	5.49
8.0	5.3	3.35	4.46
9.0	36.5	13.70	2.52
10.0	34.3	6.85	15.70
11.0	3.5	3.25	2.15
13.0	9.0	2.90	6.94
15.0	13.0	6.80	3.26
16.0	30.6	11.30	0.65
17.0	22.8	5.35	7.60
18.0	23.4	9.90	1.32
19.0	11.3	5.75	0.42
20.0	25.9	8.20	1.18
21.0	41.5	5.35	19.90
22.0	16.1	6.20	5.30
23.0	3.7	2.50	1.26

Depths are in feet, from top of core.

## TITRAMETRIC DETERMINATION OF ORGANIC CARBON WITH POTASSIUM DICHROMATE

This method is based on the oxidation of organic carbon by mixtures of chromic and sulfuric acid.

Weigh 0.1 to 0.2 gm. sample into a reaction flask, add to 10 mL of 1 N potassium dichromate and 20 mL conc.  $H_2SO_4$  to oxidize the organic carbon in sample. Then the excess dichromate is back- titrated with 0.5 N ferrous sulfate solution with barium diphenylamine as indicator.

NOTE: This analysis is not affected by carbonate or elemental carbon in the sample.

<b>WELL A</b>		25 Samples				
	TOC	RES	DENS	PORO	SONIC	GAMMA
Mean	5.22	17.92	2.459	22.8	81.0	118.1
Std. Dev.	3.71	8.43	0.107	9.07	12.2	40.9

<b>WELL B</b>		21 Samples				
	TOC	RES	DENS	PORO	SONIC	GAMMA
Mean	2.85	7.28	2.399	30.7	96.5	50.9
Std. Dev.	1.54	3.19	0.110	7.52	17.5	14.0

<b>WELL C</b>		11 Samples				
	TOC	RES	DENS	PORO	SONIC	GAMMA
Mean	3.33	11.6	2.455	32.6	96.3	110.0
Std. Dev.	1.86	21.3	0.109	3.82	15.3	47.7

<b>WELL D</b>		13 Samples				
	TOC	RES	DENS	PORO	SONIC	GAMMA
Mean	5.67	11.6	2.476	30.7	89.5	82.3
Std. Dev.	2.41	14.1	0.122	5.33	13.7	16.9

Table 1. Basic statistics for the North Sea log and TOC data.

BIVARIATE REGRESSION SUMMARY WELL A					
	RES	DENS	PORO	SONIC	GR
correlation with TOC	0.426	-0.681	0.749	0.761	0.532
regression slope	0.193	-23.63	0.310	0.232	0.048
regression offset	1.86	63.32	-1.80	-13.56	-0.481

BIVARIATE REGRESSION SUMMARY WELL B					
	RES	DENS	PORO	SONIC	GR
correlation with TOC	-0.196	-0.365	0.373	0.282	0.810
regression slope	-0.095	-5.09	0.076	0.025	0.089
regression offset	3.54	15.06	0.51	0.452	-1.674

BIVARIATE REGRESSION SUMMARY WELL C					
	RES	DENS	PORO	SONIC	GR
correlation with TOC	0.460	-0.453	0.730	0.471	0.728
regression slope	0.040	-7.73	0.356	0.058	0.029
regression offset	2.86	22.31	-8.29	-2.22	0.191

BIVARIATE REGRESSION SUMMARY WELL D					
	RES	DENS	PORO	SONIC	GR
correlation with TOC	-0.029	-0.574	0.797	0.882	0.781
regression slope	-0.005	-11.31	0.361	0.155	0.112
regression offset	5.73	33.69	-5.42	-8.24	-3.52

BIVARIATE REGRESSION SUMMARY ALL WELLS COMBINED					
	RES	DENS	PORO	SONIC	GR
correlation with TOC	0.305	-0.372	0.399	0.305	0.557
regression slope	0.072	-9.51	0.140	0.055	0.037
regression offset	3.38	27.53	0.321	-0.67	0.91

Table 2. Summary of bivariate regression results for the North Sea wells.

**CORRELATION MATRIX WELL A**

	RES	DENS	PORO	SONIC	GR	TOC
RES	1.0	-0.359	0.632	0.448	0.641	0.426
DENS		1.0	-0.742	-0.750	-0.673	-0.681
PORO			1.0	0.798	0.893	0.749
SONIC				1.0	0.687	0.761
GR					1.0	0.532
TOC						1.0

**CORRELATION MATRIX WELL B**

	RES	DENS	PORO	SONIC	GR	TOC
RES	1.0	0.595	-0.646	-0.661	-0.170	-0.196
DENS		1.0	-0.909	-0.895	-0.186	-0.365
PORO			1.0	0.926	0.222	0.373
SONIC				1.0	0.044	0.282
GR					1.0	0.810
TOC						1.0

**CORRELATION MATRIX WELL C**

	RES	DENS	PORO	SONIC	GR	TOC
RES	1.0	0.341	0.272	-0.396	-0.100	0.460
DENS		1.0	-0.570	-0.723	-0.696	-0.453
PORO			1.0	0.385	0.570	0.730
SONIC				1.0	0.866	0.471
GR					1.0	0.728
TOC						1.0

**CORRELATION MATRIX WELL D**

	RES	DENS	PORO	SONIC	GR	TOC
RES	1.0	-0.183	0.258	-0.403	-0.046	-0.029
DENS		1.0	-0.764	-0.426	-0.258	-0.574
PORO			1.0	0.618	0.536	0.797
SONIC				1.0	0.675	0.882
GR					1.0	0.781
TOC						1.0

Tables 3A-D. Correlation matrices for TOC and log responses from the North Sea wells.

<b>ANALYSIS OF VARIANCE WELL A</b>						
Source of variation	Sum of squares	Degrees of freedom	Mean squares	F test	R <sub>M</sub>	Goodness of fit
Regression	230.38	4	57.603	12.573 <sup>a</sup>	0.852	0.726
Deviation	87.04	19	4.580			
Total	317.41	23				

<sup>a</sup>Significant at the 99% acceptance level.

<b>ANALYSIS OF VARIANCE WELL B</b>						
Source of variation	Sum of squares	Degrees of freedom	Mean squares	F test	R <sub>M</sub>	Goodness of fit
Regression	34.56	4	8.643	10.694 <sup>a</sup>	0.853	0.728
Deviation	12.93	16	0.811			
Total	47.48	20				

<sup>a</sup>Significant at the 99% acceptance level.

<b>ANALYSIS OF VARIANCE WELL C</b>						
Source of variation	Sum of squares	Degrees of freedom	Mean squares	F test	R <sub>M</sub>	Goodness of fit
Regression	25.80	4	6.456	4.266 <sup>a</sup>	0.860	0.734
Deviation	9.07	6	1.512			
Total	34.87	10				

<sup>a</sup>Significant at the 95% acceptance level.

<b>ANALYSIS OF VARIANCE WELL D</b>						
Source of variation	Sum of squares	Degrees of freedom	Mean squares	F test	R <sub>M</sub>	Goodness of fit
Regression	64.33	4	16.087	22.695 <sup>a</sup>	0.959	0.919
Deviation	5.67	8	0.715			
Total	69.98	12				

<sup>a</sup>Significant at the 99% acceptance level.

Tables 4A-D. ANOVA results for regressions of TOC on the log responses, from the North Sea wells.



**CORRELATION MATRIX ALL NORTH SEA WELL DATA**

	RES	DENS	PORO	SONIC	GR	TOC
RES	1.0	0.077	0.032	-0.290	0.328	0.305
DENS		1.0	-0.673	-0.703	-0.213	-0.372
PORO			1.0	0.783	0.201	0.399
SONIC				1.0	0.135	0.305
GR					1.0	0.558
TOC						1.0

<b>ANALYSIS OF VARIANCE ALL NORTH SEA WELL DATA</b>						
Source of variation	Sum of squares	Degrees of freedom	Mean squares	F test	R <sub>M</sub>	Goodness of fit
Regression	230.83	4	57.713	10.922 <sup>a</sup>	0.637	0.406
Deviation	338.15	64	5.280			
Total	568.97	68				

<sup>a</sup>Significant at the 99% acceptance level.

Table 5. Correlation matrix and ANOVA results for multiple regression, from all North Sea well data combined.

	Regression Equation 8-A	Regression Equation 8-B	Regression Equation 8-C	Regression Equation 8-D
Well A Data	0.852	0.550	0.598	0.714
Well B Data	0.224	0.853	0.660	0.482
Well C Data	0.023	0.685	0.860	0.697
Well D Data	0.790	0.827	0.648	0.958

Table 6. Matrix of "cross-regression" correlation coefficients. These are the correlation coefficients between TOC's predicted by the specified equations, and the actual values. The diagonal elements are the multiple correlation coefficients obtained from the data which constrained the regressions.

	Regression Equation 8-A	Regression Equation 8-B	Regression Equation 8-C	Regression Equation 8-D
Well A Data	1.58	4.26	3.19	2.30
Well B Data	11.11	0.63	2.21	2.64
Well C Data	7.52	5.08	0.83	4.39
Well D Data	5.27	1.13	3.41	0.52

Table 7. Matrix of "mean-square differences" demonstrates the utility of the various regression equations when applied to data which did not constrain them. The diagonal elements are the best results achievable with a linear equation. (See Text and Equation 10).

BIVARIATE REGRESSION SUMMARY			
	Correlation with TOC	Regression slope	Regression offset
RES	-0.151	-0.105	11.643
DENS	-0.330	-7.350	25.402
PORO	-0.353	-0.566	25.162
SONIC	0.493	0.188	-8.186
GAMMA	0.650	0.040	2.618
URAN	0.562	0.121	4.497
THOR	0.614	0.552	4.787
POTA	0.341	1.892	6.690

Table 8. Summary of bivariate regression relationships for TOC and log data, from the California well.

**CORRELATION MATRIX, CALIFORNIA WELL, TOC AND WELL LOGS**

	RES	DENS	PORO	SONIC	GAMMA	THOR	URAN	POTA	TOC
RES	1.000	0.178	0.299	-0.145	0.044	-0.101	0.029	0.201	-0.151
DENS		1.000	-0.002	-0.713	0.141	-0.440	0.183	0.060	-0.330
PORO			1.000	-0.131	-0.032	-0.303	0.070	0.288	-0.358
SONIC				1.000	0.043	0.728	-0.071	-0.049	0.493
GAMMA					1.000	0.116	0.953	0.763	0.650
THOR						1.000	-0.042	0.039	0.641
URAN							1.000	0.714	0.562
POTA								1.000	0.341
TOC									1.000

**CORRELATION MATRIX, CALIFORNIA WELL, BITUMEN AND WELL LOGS**

	RES	DENS	PORO	SONIC	GAMMA	THOR	URAN	POTA	BIT
RES	1.000	0.178	0.299	-0.145	0.044	-0.101	0.029	0.201	-0.229
DENS		1.000	-0.002	-0.713	0.141	-0.440	0.183	0.060	0.638
PORO			1.000	-0.131	-0.032	-0.303	0.070	0.288	-0.222
SONIC				1.000	0.043	0.728	-0.071	-0.049	-0.422
GAMMA					1.000	0.116	0.953	0.763	0.429
THOR						1.000	-0.042	0.039	-0.221
URAN							1.000	0.714	0.433
POTA								1.000	0.120
BIT									1.000

**CORRELATION MATRIX, CALIFORNIA WELL, BFOC AND WELL LOGS**

	RES	DENS	PORO	SONIC	GAMMA	THOR	URAN	POTA	BFOC
RES	1.000	0.178	0.299	-0.145	0.044	-0.101	0.029	0.201	-0.077
DENS		1.000	-0.002	-0.713	0.141	-0.440	0.183	0.060	-0.536
PORO			1.000	-0.131	-0.032	-0.303	0.070	0.288	-0.282
SONIC				1.000	0.043	0.728	-0.071	-0.049	0.629
GAMMA					1.000	0.116	0.953	0.763	0.513
THOR						1.000	-0.042	0.039	0.713
URAN							1.000	0.714	0.423
POTA								1.000	0.303
BFOC									1.000

Tables 9-11. Correlation matrices for the California well. TOC, Bitumen, and Bitumen-free organic carbon versus the well logs.

ANALYSIS OF VARIANCE CALIFORNIA WELL						
Source of variation	Sum of squares	Degrees of freedom	Mean squares	F test	R <sub>M</sub>	Goodness of fit
Regression	155.33	7	22.190	22.190 <sup>a</sup>	0.927	0.859
Deviation	25.52	33	0.773			
Total	180.85	40				

<sup>a</sup>Significant at the 99% acceptance level.

ANALYSIS OF VARIANCE CALIFORNIA LIMITED REGRESSION						
Source of variation	Sum of squares	Degrees of freedom	Mean squares	F test	R <sub>M</sub>	Goodness of fit
Regression	134.25	4	33.56	25.916 <sup>a</sup>	0.861	0.742
Deviation	46.62	36	1.30			
Total	180.85	40				

<sup>a</sup>Significant at the 99% acceptance level.

Table 12. ANOVA results for regressions of the log responses on TOC, for the California Well.

	Regres. Eqn. 8-A	Regres. Eqn. 8-B	Regres. Eqn. 8-C	Regres. Eqn. 8-D	Calif. Regres.
Well A Data	0.852	0.550	0.598	0.714	-0.574
Well B Data	0.224	0.853	0.660	0.482	-0.120
Well C Data	0.023	0.685	0.860	0.697	0.327
Well D Data	0.790	0.827	0.648	0.958	0.024
Calif. Data	-0.432	0.704	0.348	0.743	0.862

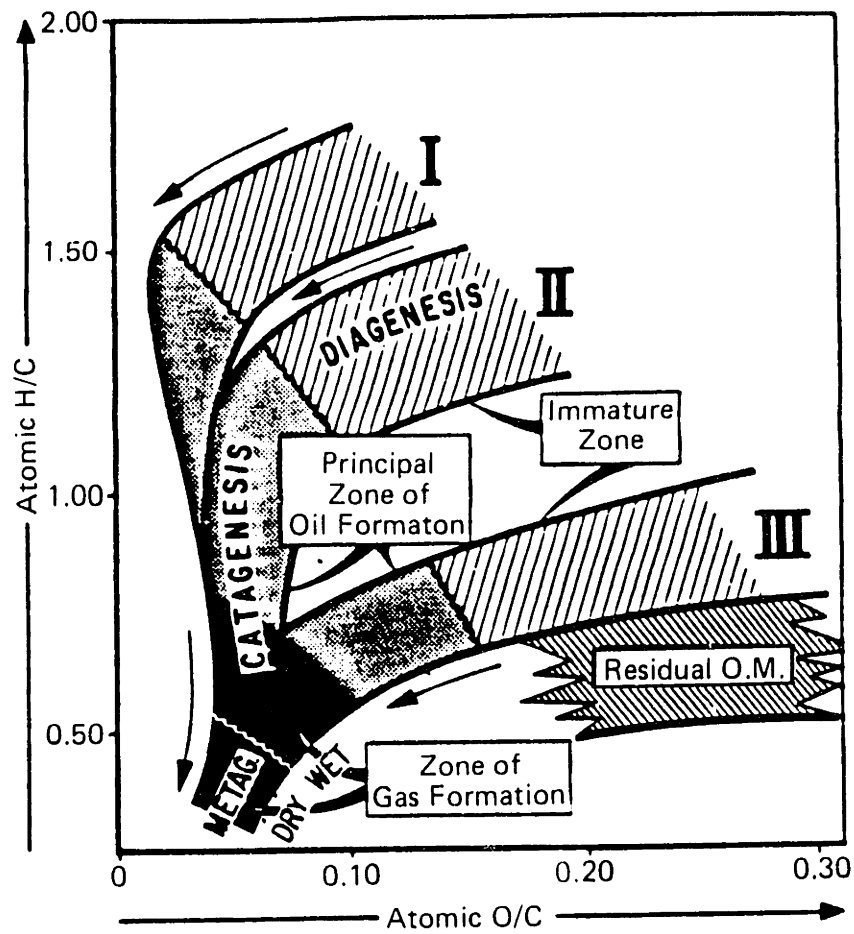
Table 13. Matrix of "cross-regression" correlation coefficients for California and North Sea wells. The diagonal elements are the multiple correlation coefficients obtained from the data which constrained that regression. The upper left 4x4 sub-matrix is identical to Table 6.

	Regres. Eqn. 8-A	Regres. Eqn. 8-B	Regres. Eqn. 8-C	Regres. Eqn. 8-D	Calif. Regres.
Well A Data	1.58	4.26	3.19	2.30	3.91
Well B Data	11.11	0.63	2.21	2.64	2.06
Well C Data	7.52	5.08	0.83	4.39	2.03
Well D Data	5.27	1.14	3.41	0.52	4.56
Calif. Data	4.15	5.67	6.11	1.22	0.88

Table 14. Elements of the "mean square difference" matrix are the square root of the squared difference between actual TOC's and those from a predictive equation. The diagonal elements represent the minimum difference achievable. The upper left 4x4 sub-matrix is identical to Table 7.

	WELL A	WELL B	WELL C	WELL D	CALIF. WELL
$\rho_{ma}$ , gm/cc	2.70	2.80	2.85	2.75	2.65
$\Delta t_{ma}$ , $\mu$ sec/ft	65	85	80	68	65
$\Phi$ , % Vol.	6	25	23	15	10
$\Delta t_{ker}$ , $\mu$ sec/ft	180	300	330	180	170
$\rho_{ker}$ , gm/cc	1.0	1.0	1.0	1.0	1.0
$HI_{ker}$ , atoms/atoms	0.67	0.67	0.67	0.67	0.67

Table 15. Matrix parameters used to construct the volumetric log response models, for each well studied.



Principal Products of Kerogen Evolution





-  CO<sub>2</sub>, H<sub>2</sub>O
-  Oil
-  Gas
-  Residual Organic Matter  
(No Potential for Oil or Gas)

Figure 1. Van Krevelen Diagram showing types of kerogen, and principal products generated during thermal evolution of Types I, II, and III kerogen. Residual organic matter has no real potential for petroleum and no real evolution path (after Tissot et. al., 1982).



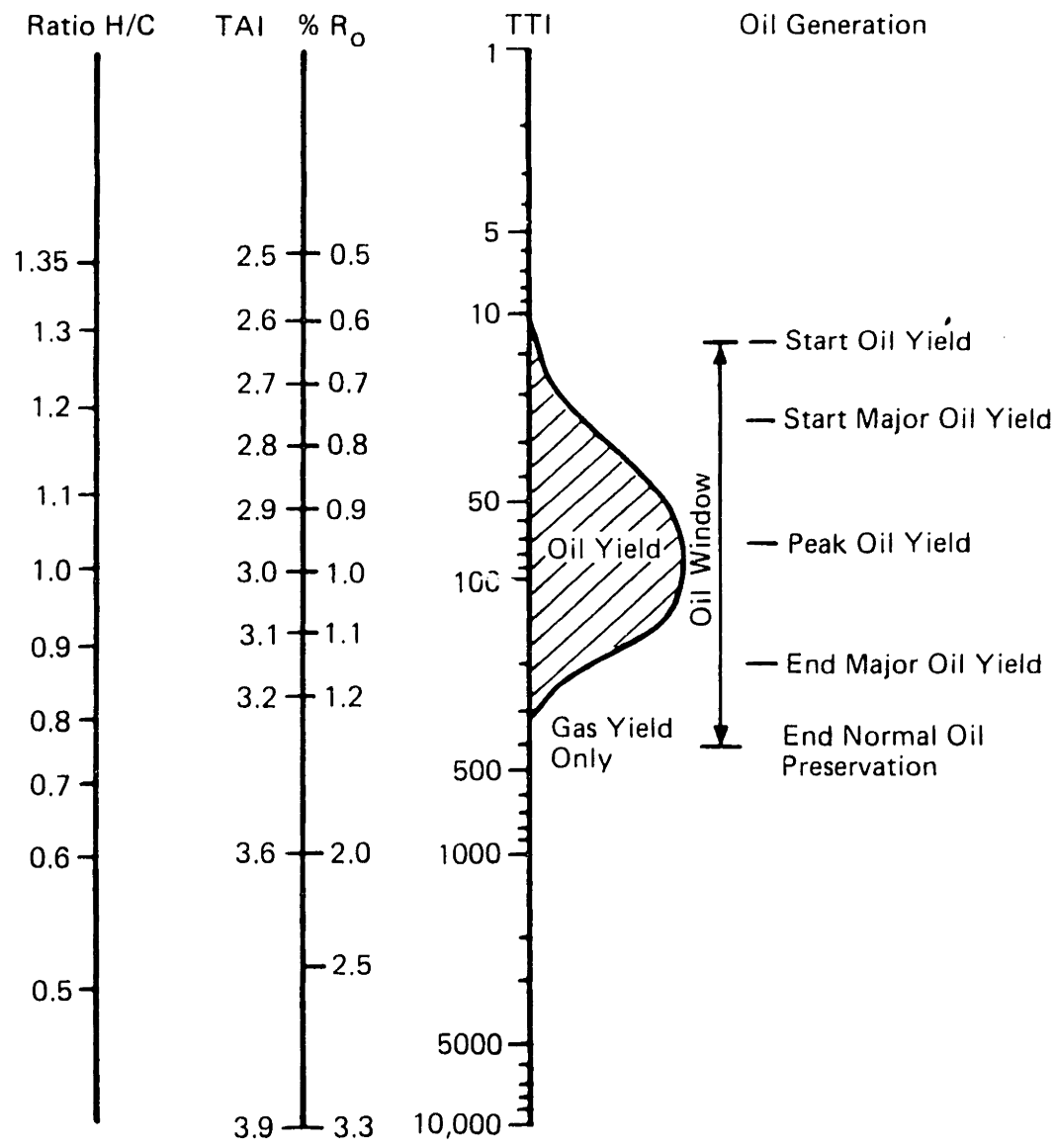


Figure 2. Relation between some different maturity indicators and probable periods of hydrocarbon generation. TAI is thermal alteration index,  $R_0$  is vitrinite reflectance, and TTI is time-temperature index (after Ayres et. al., 1982).

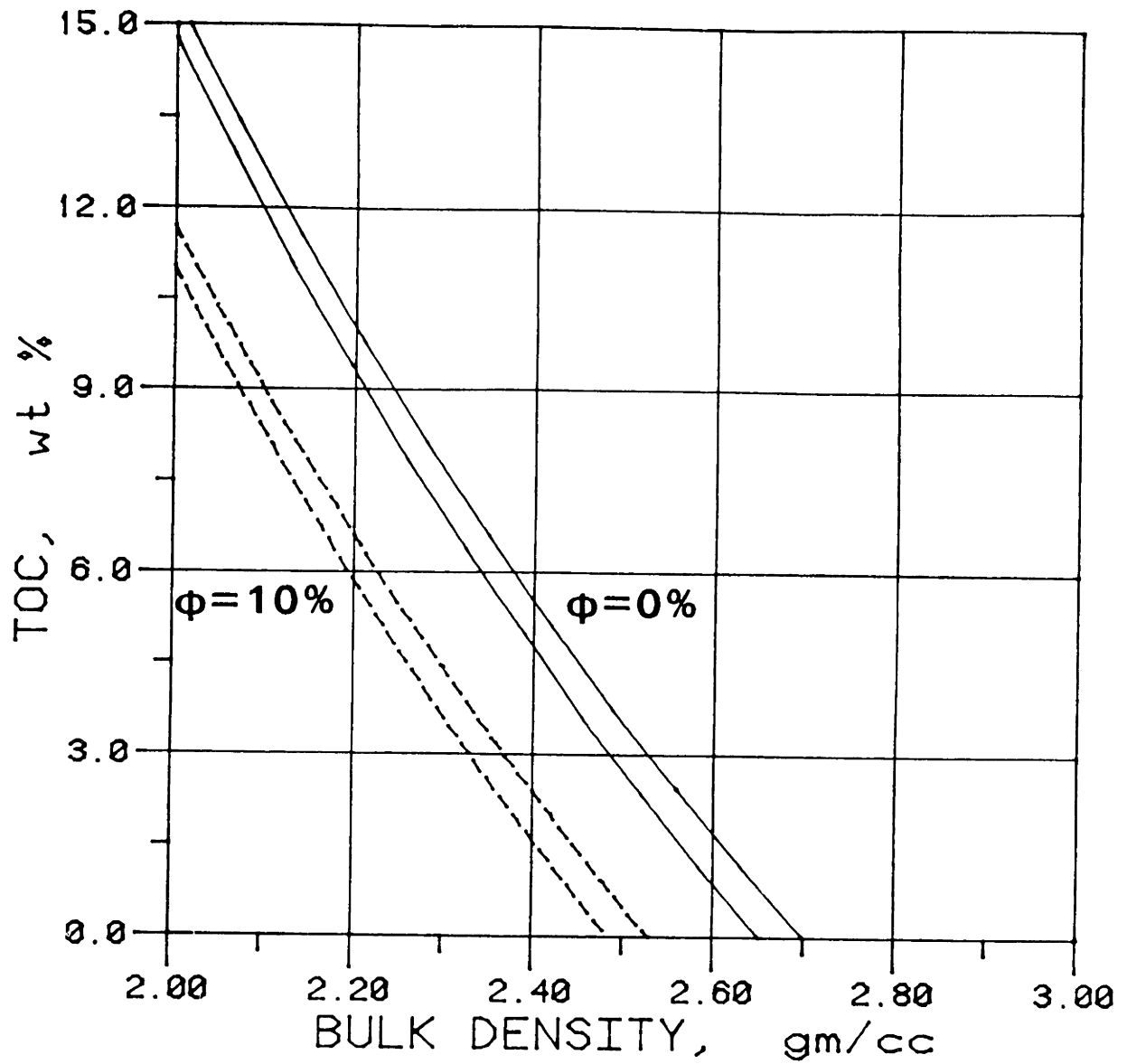


Figure 3. Calculated volumetric average response of density log to organic matter content, expressed in terms of total organic carbon (TOC). For each porosity ( $\phi=0$  and  $\phi=10$ ) the effect of modelling with matrix densities of 2.65 and 2.70 g/cc is shown.

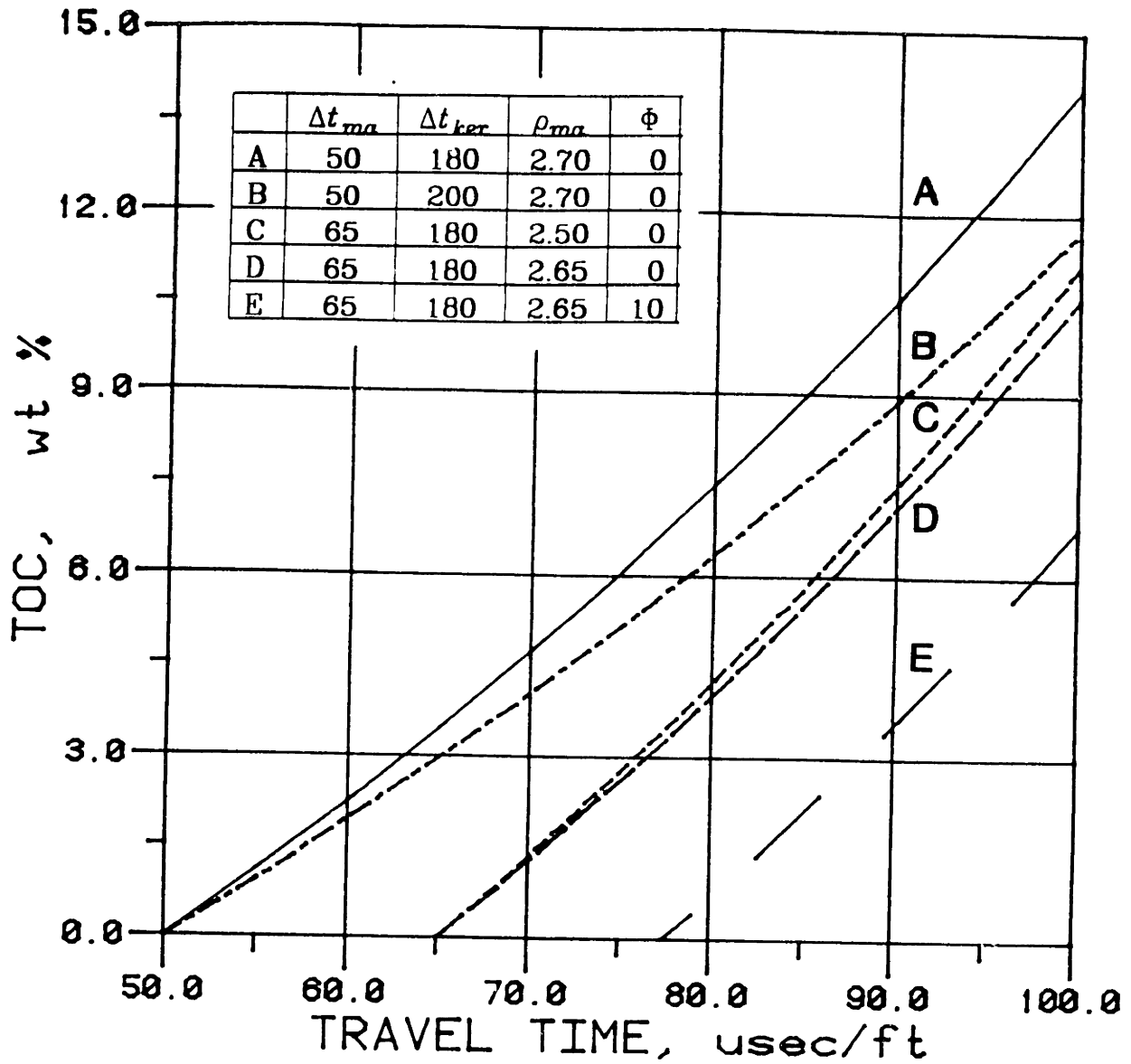


Figure 4. Calculated volumetric average response of sonic log to organic matter content. Curves A, B, C, and D are based on two component models ( $\phi=0\%$ ). Curve E is a three component model with  $\phi=10\%$  porosity, and the pore space filled with water.

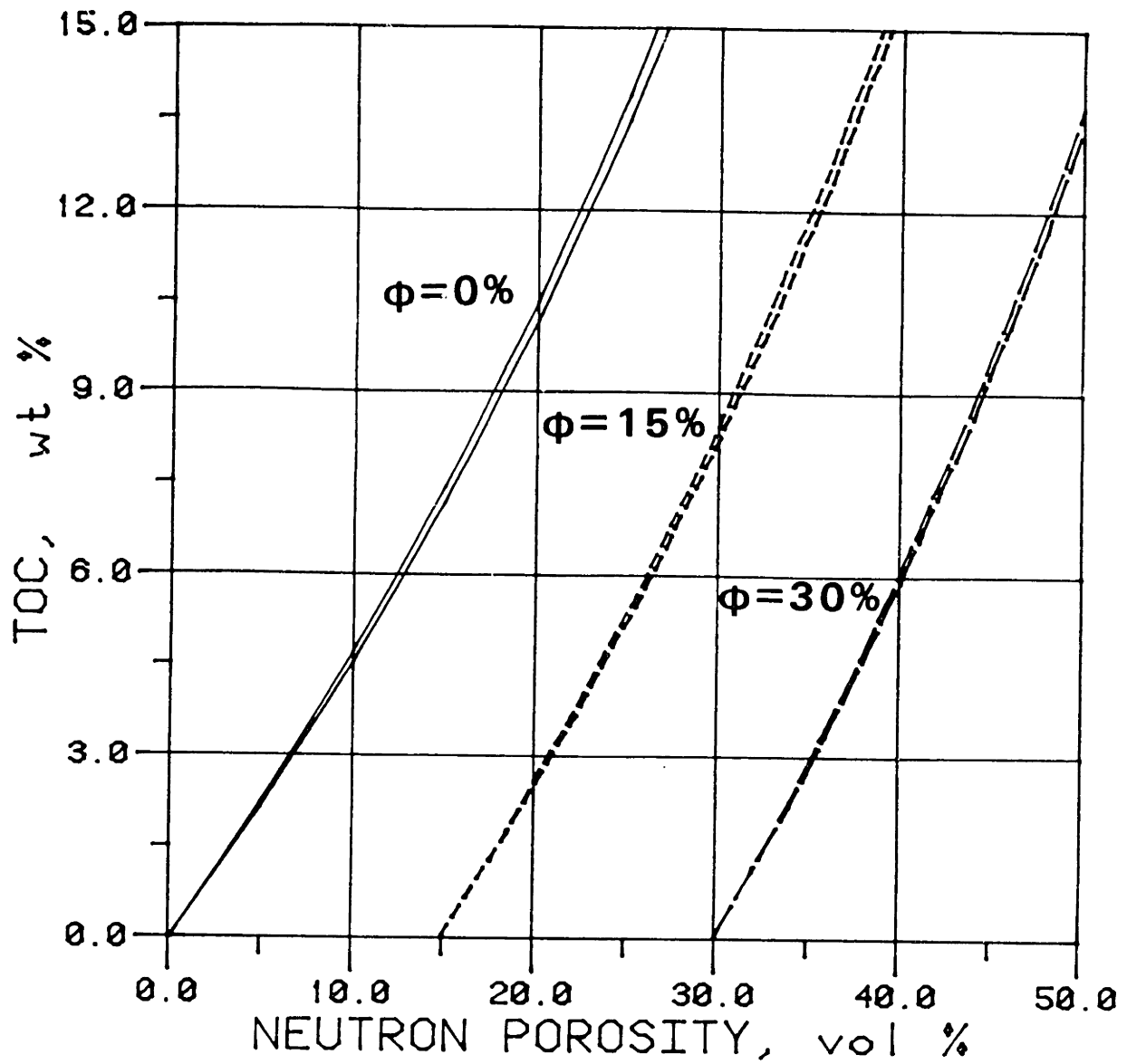


Figure 5. Calculated volumetric average response of neutron log to organic matter content using three component models. Curves are shown for 0, 15, and 30 percent porosity formations. Matrix densities used in the solutions are 2.65 for the leftmost line, 2.70 g/cc for the rightmost line of each pair.

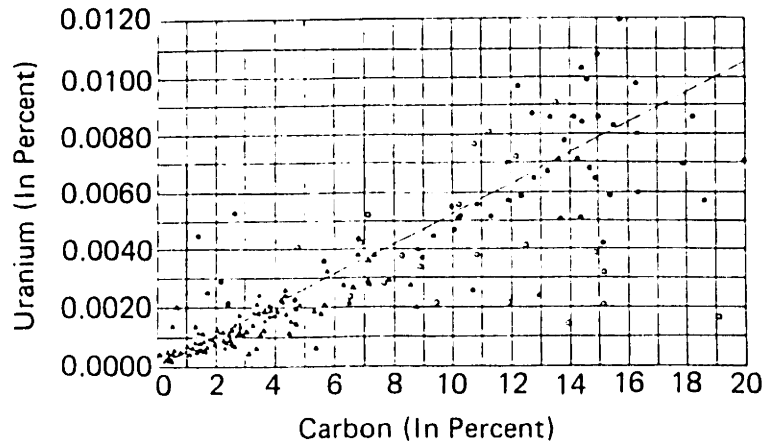


Figure 6. Organic carbon versus uranium in Appalachian Devonian Black Shale samples. Solid circles and lines of correlation represent data from Swanson (1960); triangles show data from Leventhal, 1979; open circles show data from Leventhal, 1980; (after Leventhal, 1983).

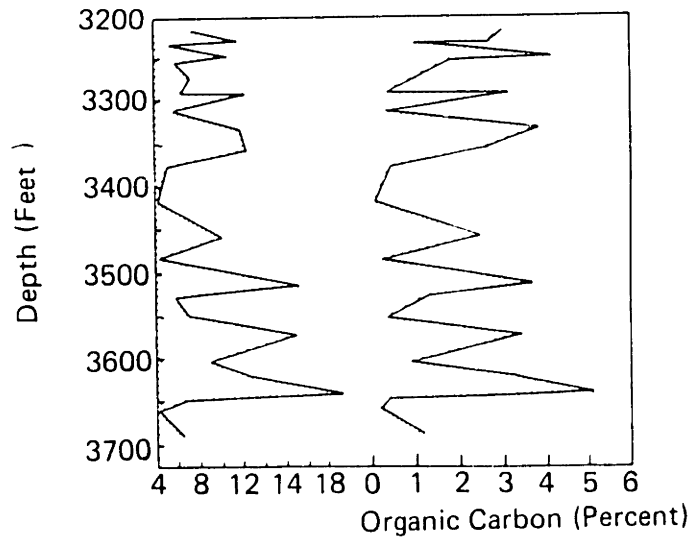


Figure 7. Variations in uranium and TOC in Devonian Black Shales, Jackson County, West Virginia, (Fertl, 1979).

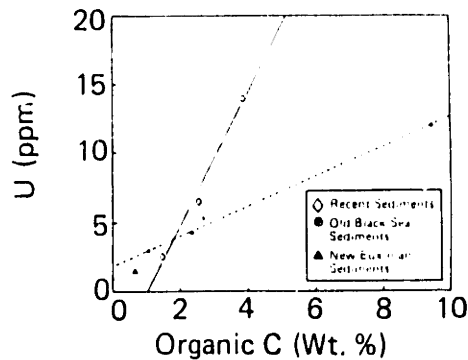


Figure 8. Correlation between uranium and organic carbon in some sediments from the Black Sea (After Calvert, 1976).

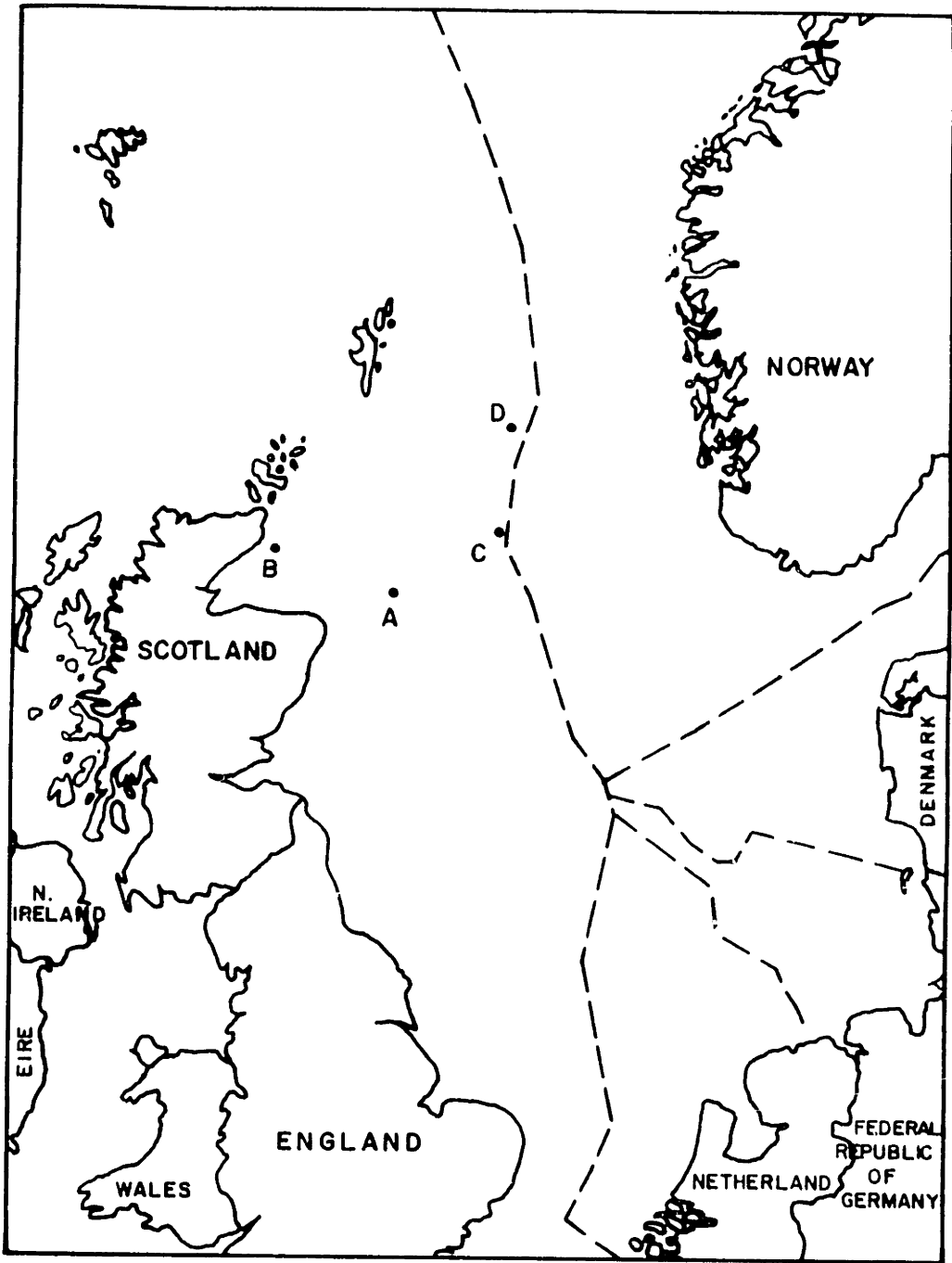
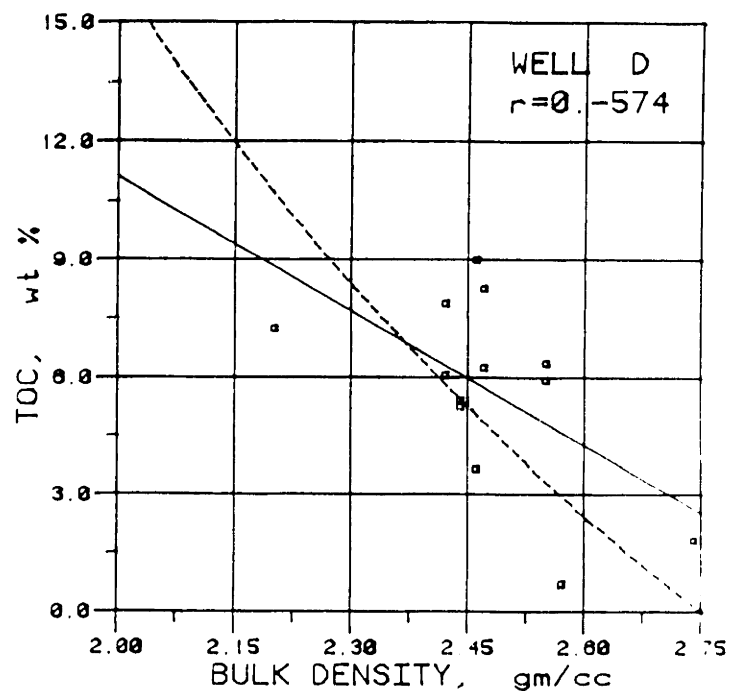
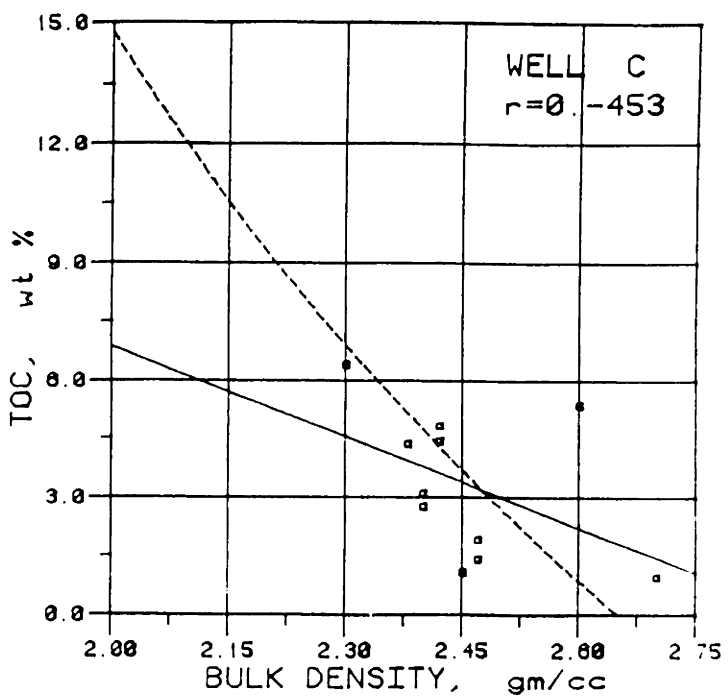
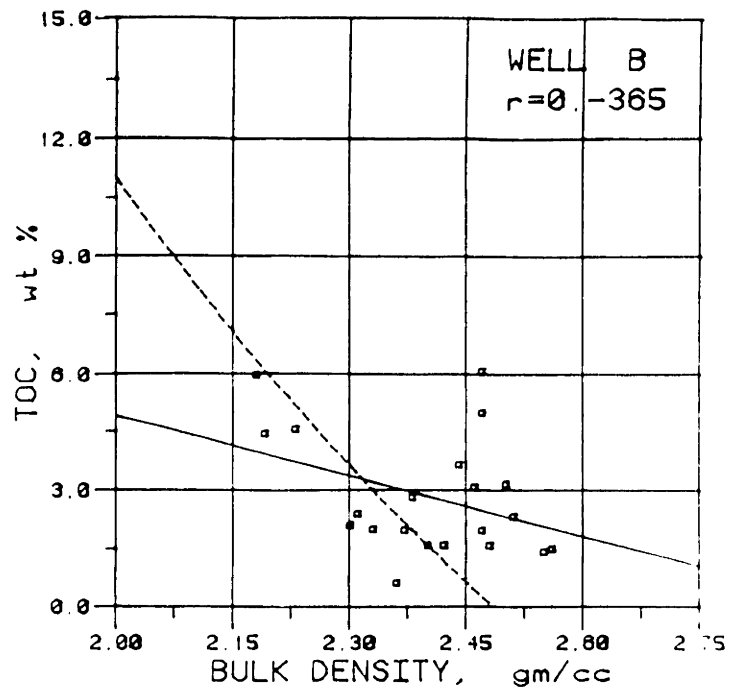
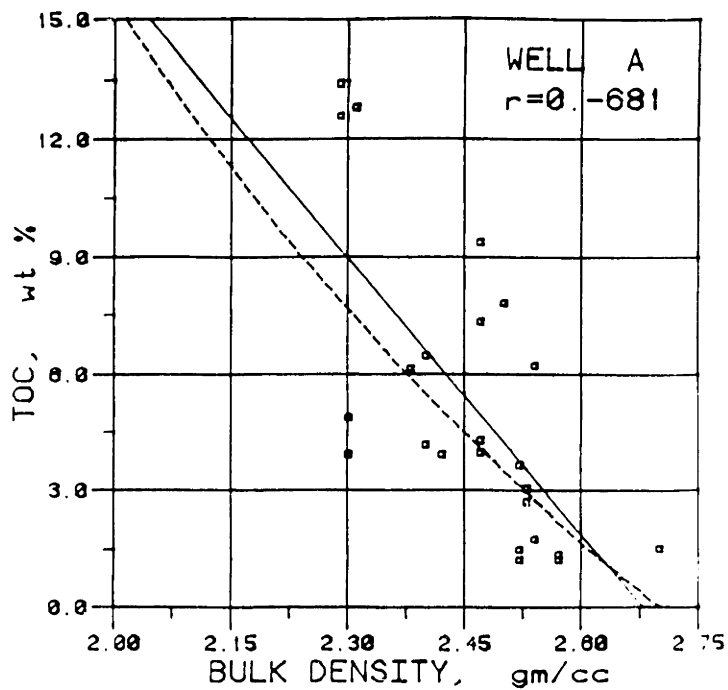
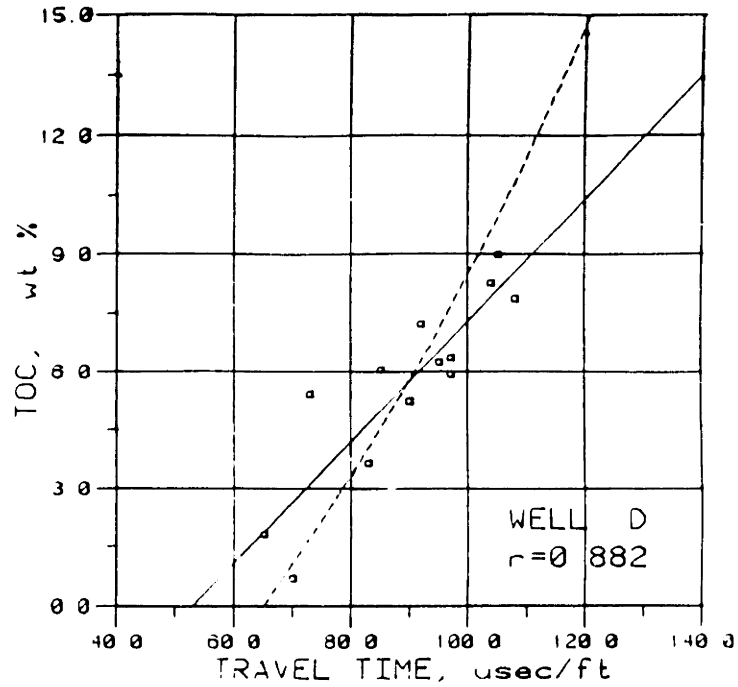
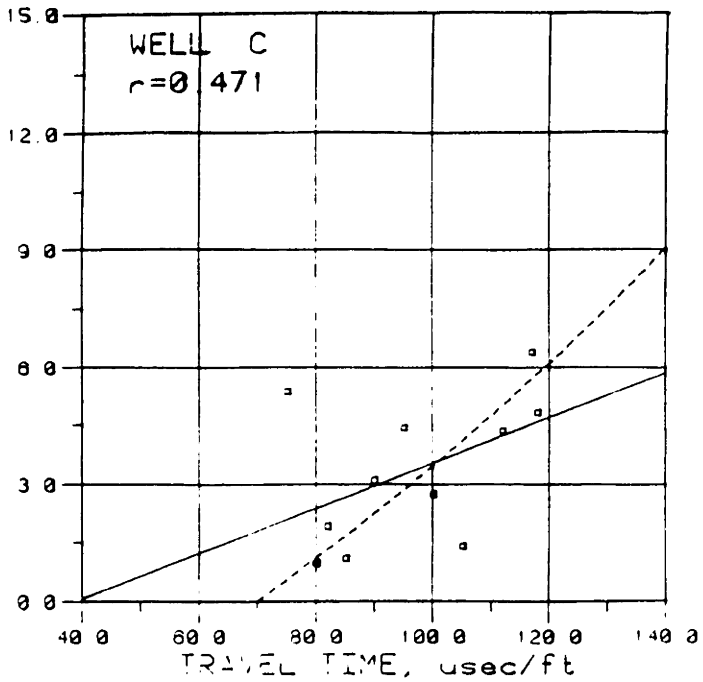
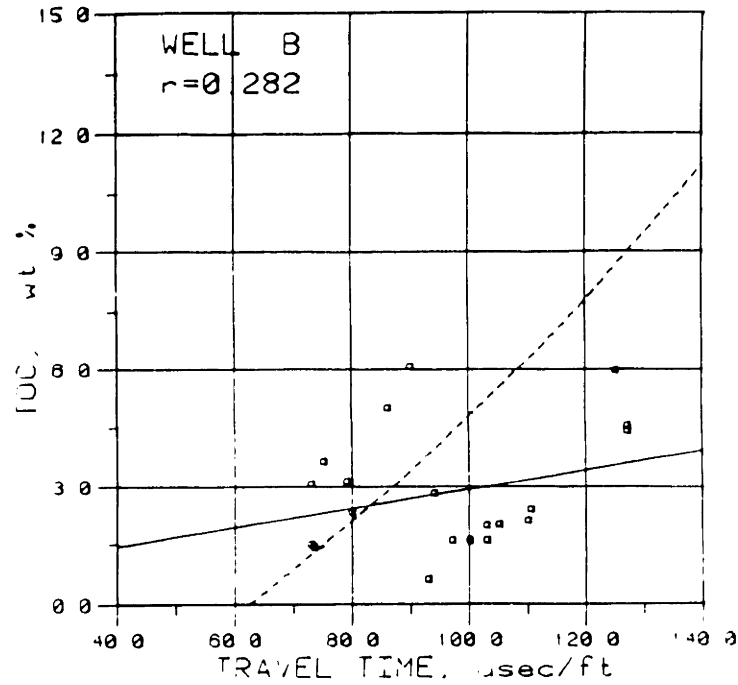
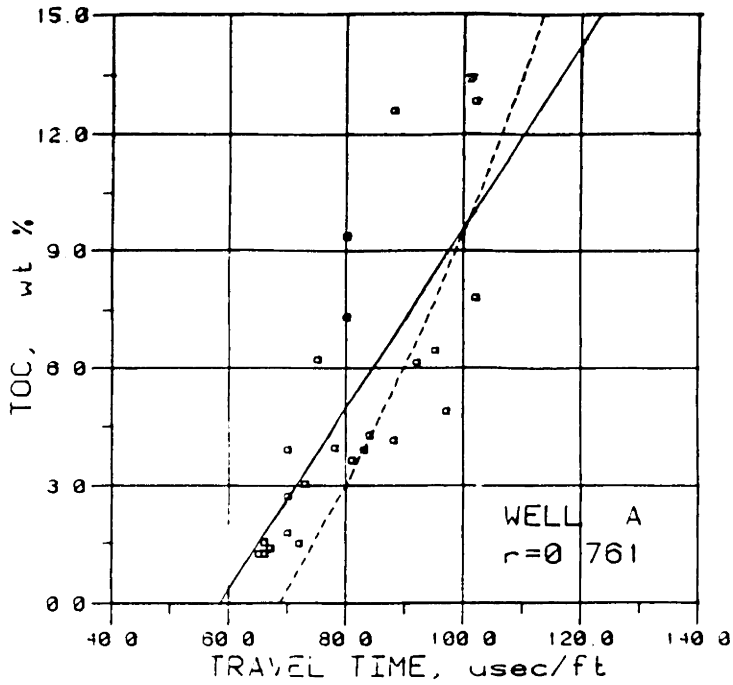


Figure 9. Map showing approximate locations of the four North Sea Wells.

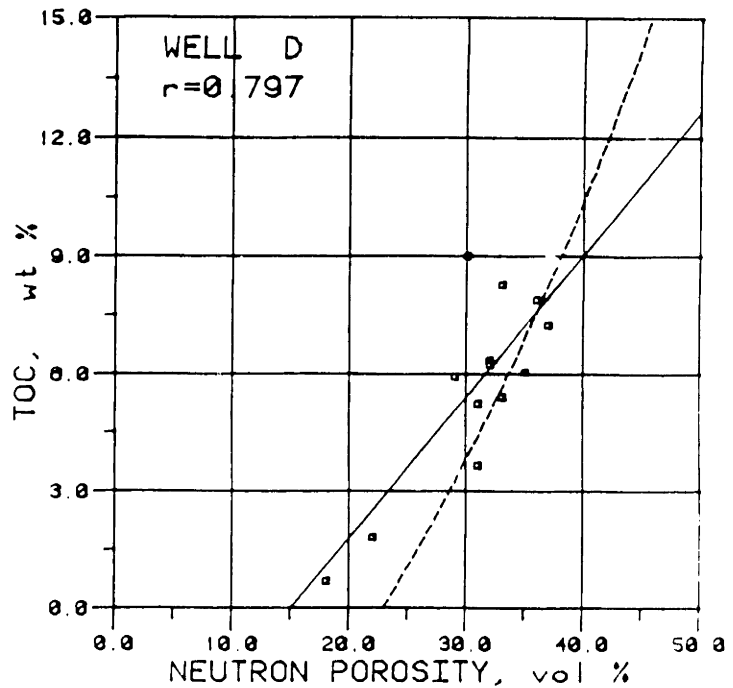
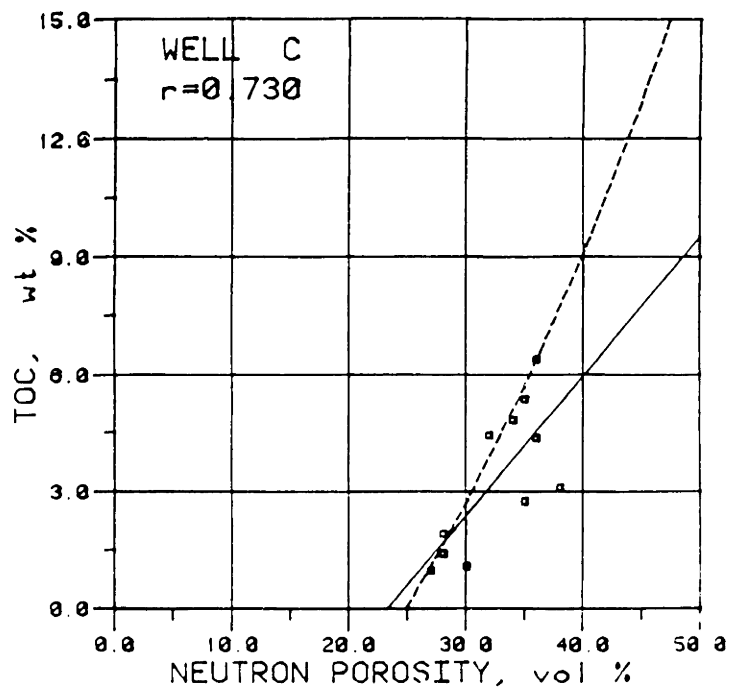
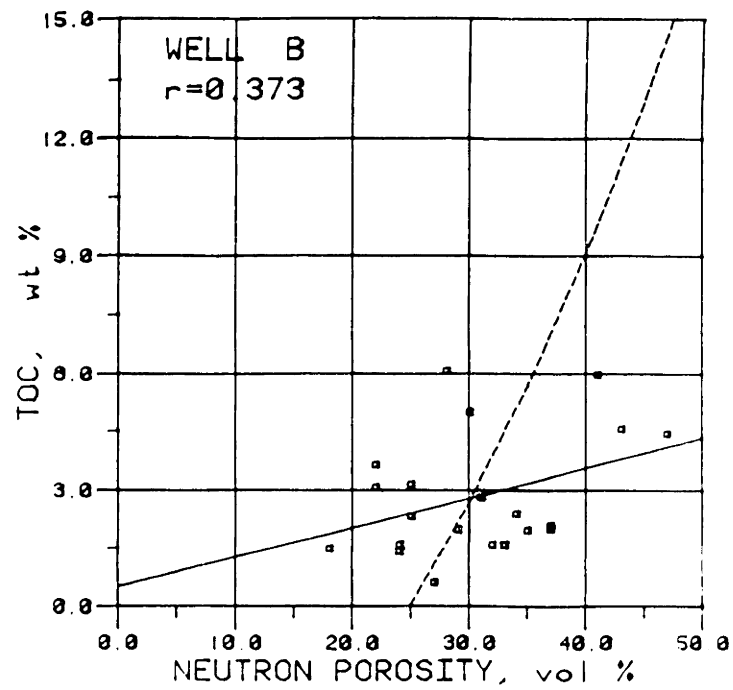
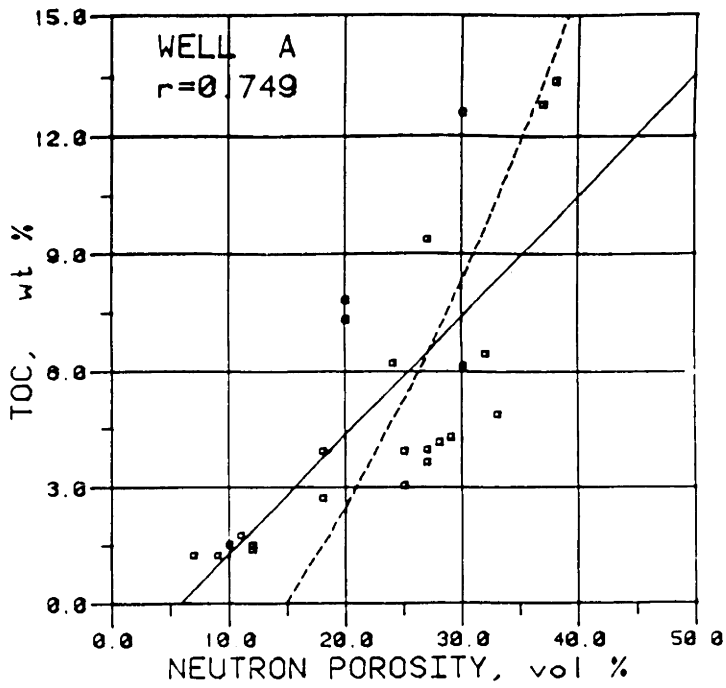


Figures 10A-D. Plots of TOC versus apparent bulk density for the four North Sea wells. Solid lines indicate least squares regression results. Dashed lines are the log responses predicted by volumetric averaging. Parameters used to construct the models are listed in Table 14.

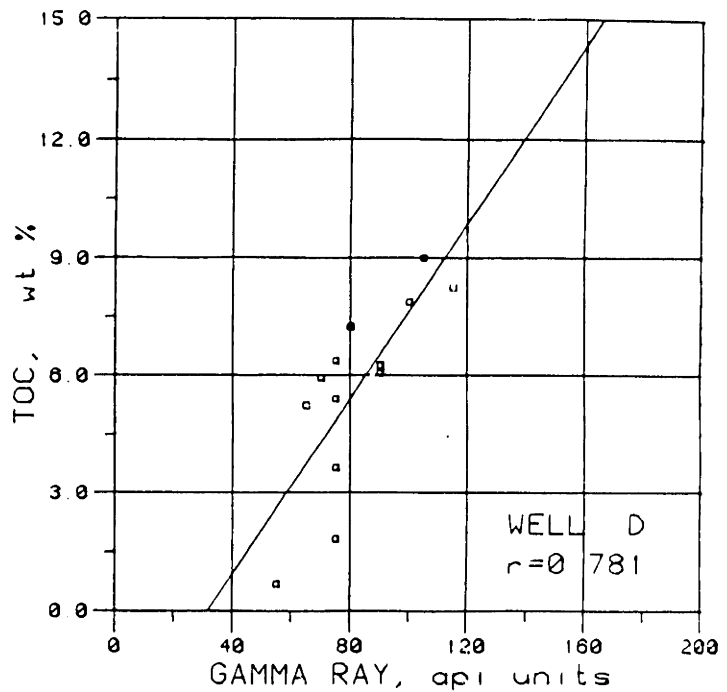
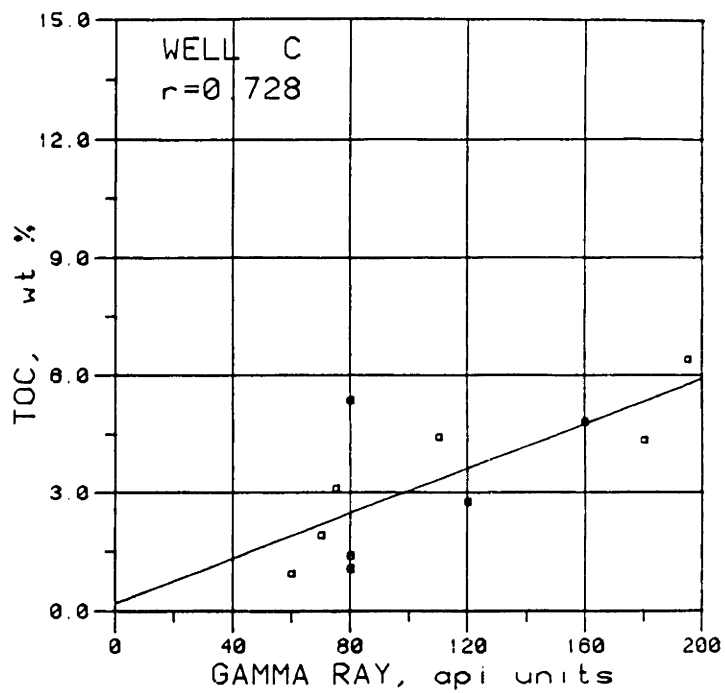
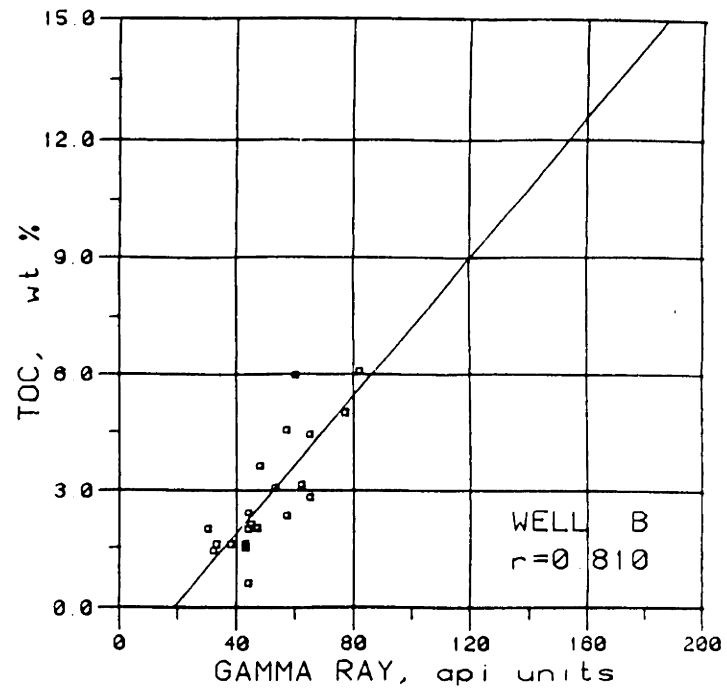
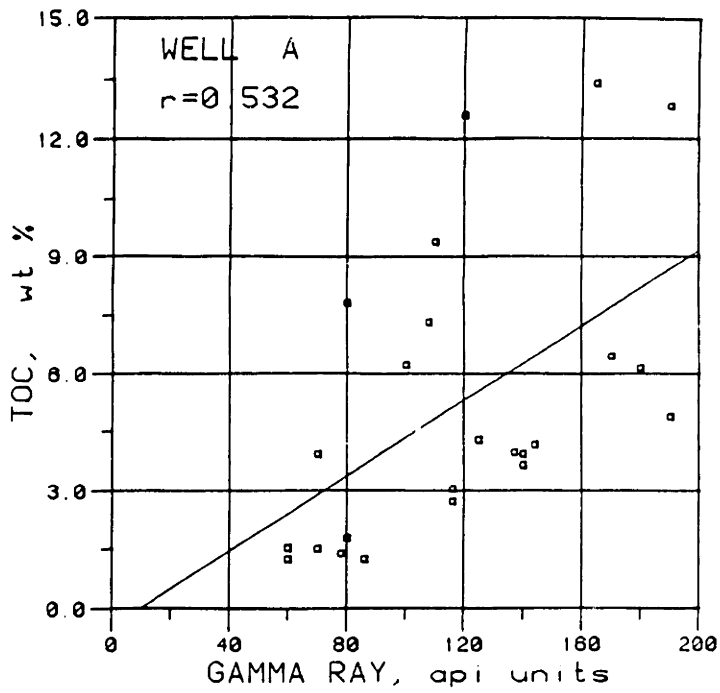


Figures 11A-D. Plots of TOC versus sonic travel time for the four North Sea wells. Solid lines indicate least squares regression results. Dashed lines are the log responses predicted by volumetric averaging. Parameters used to construct the models are listed in Table 14.

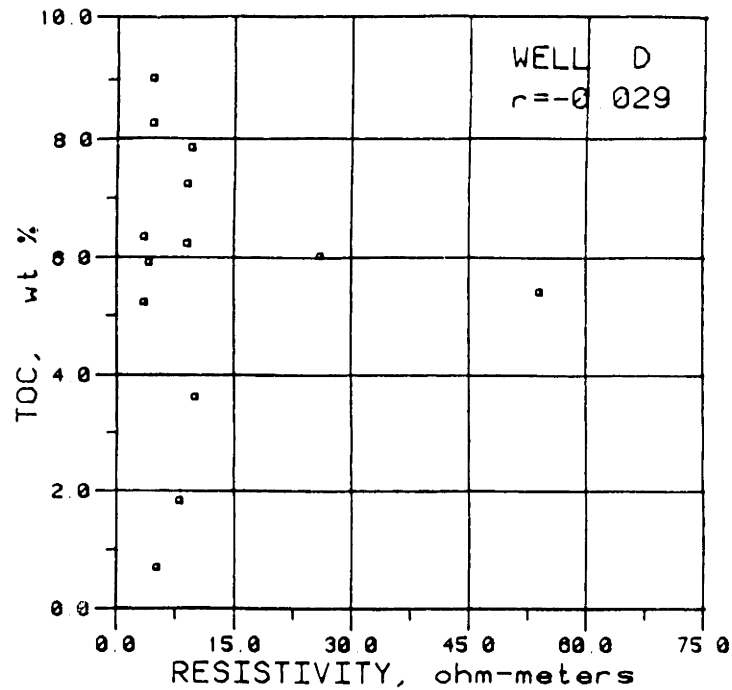
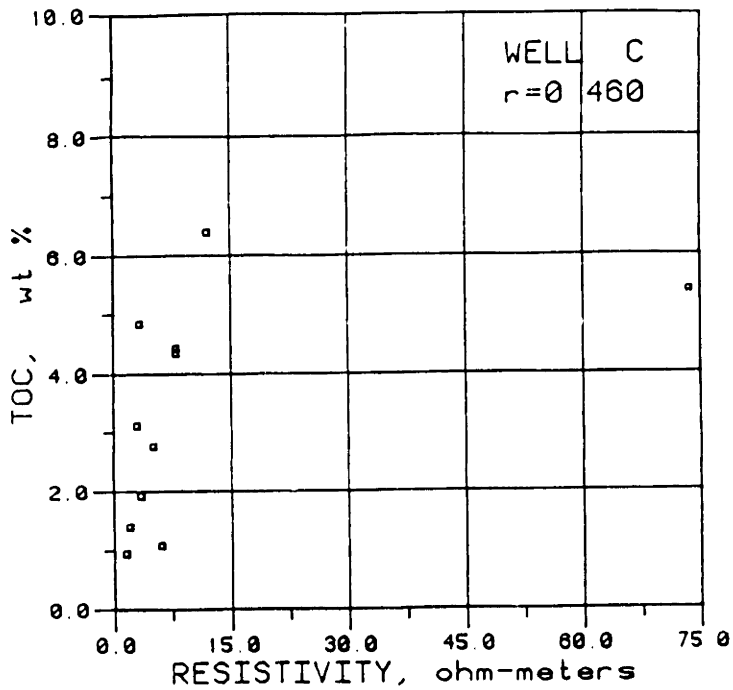
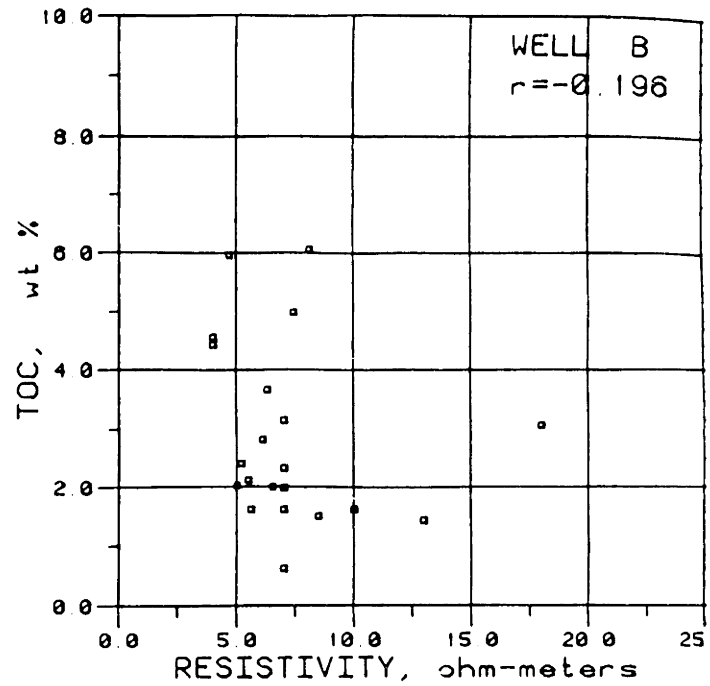
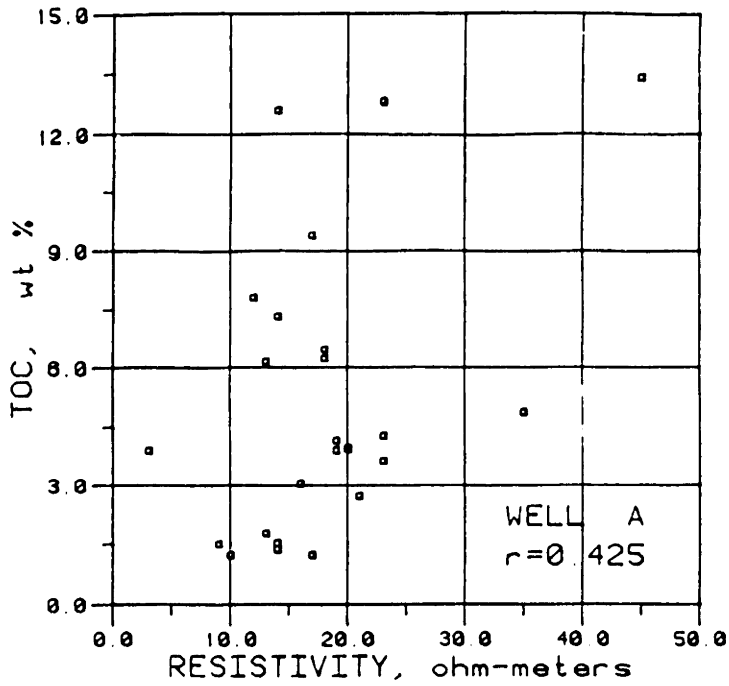




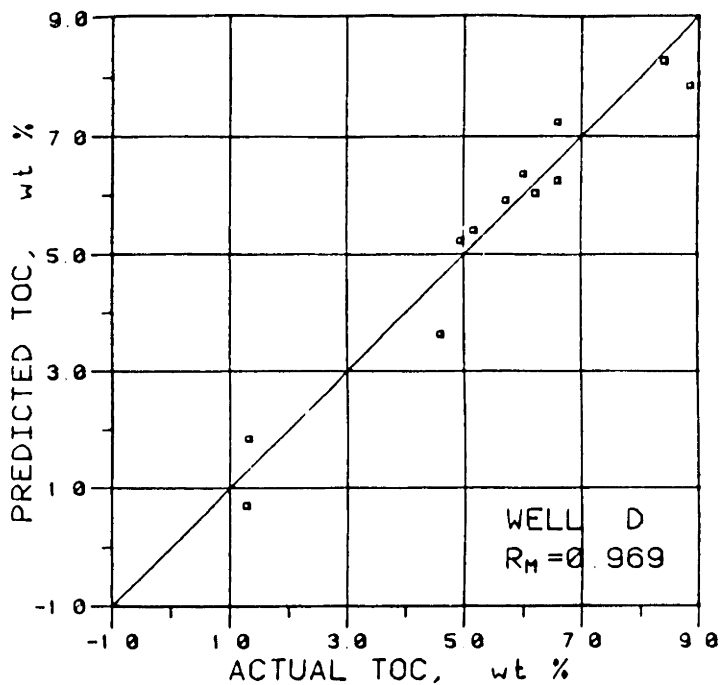
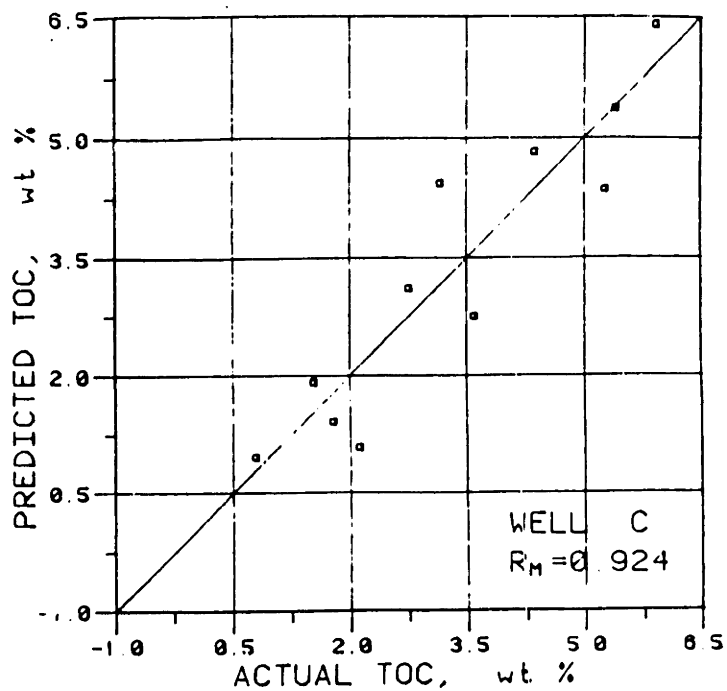
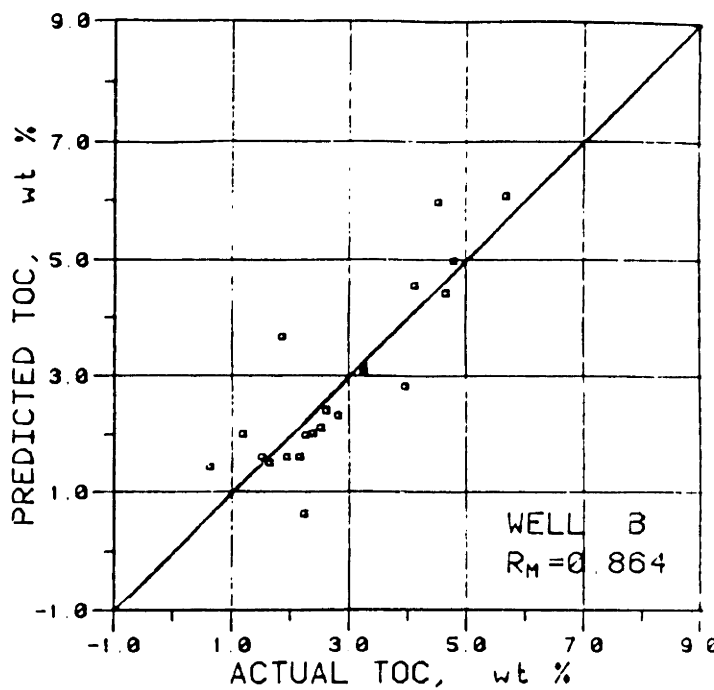
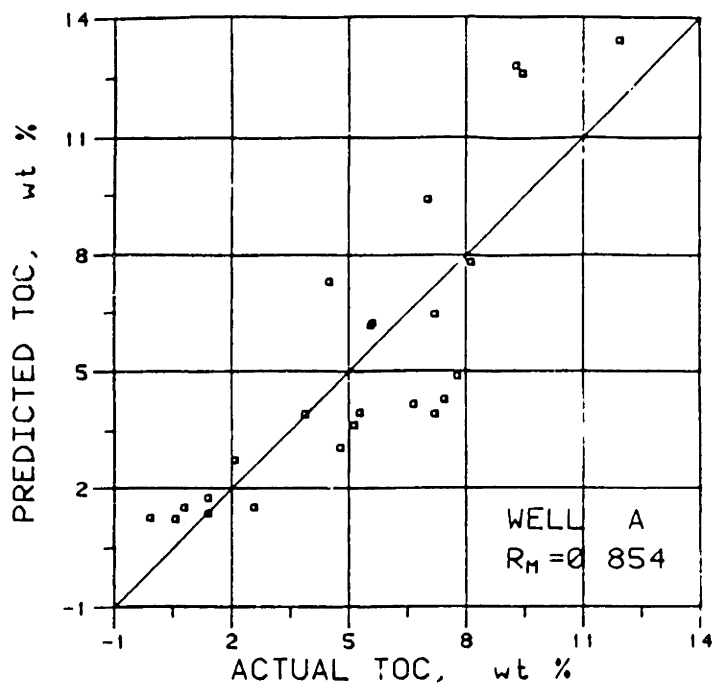
Figures 12A-D. Plots of TOC versus apparent neutron porosity for the four North Sea wells. Solid lines indicate least squares regression results. Dashed lines are the log responses predicted by volumetric averaging. Parameters used to construct the models are listed in Table 14.



Figures 13A-D. Plots of TOC versus total gamma ray intensity for the four North Sea wells. Solid lines indicate least squares regression results.



Figures 14A-D. Crossplots of TOC versus resistivity log for the four North Sea wells. Because kerogen does not replace water in the rock, resistivity is not a TOC indicator.



Figures 15A-D. Plots show the fit of TOC's calculated by multiple regression for each North Sea well.  $R_M$ , the multiple correlation coefficient, is the square root of goodness of fit.

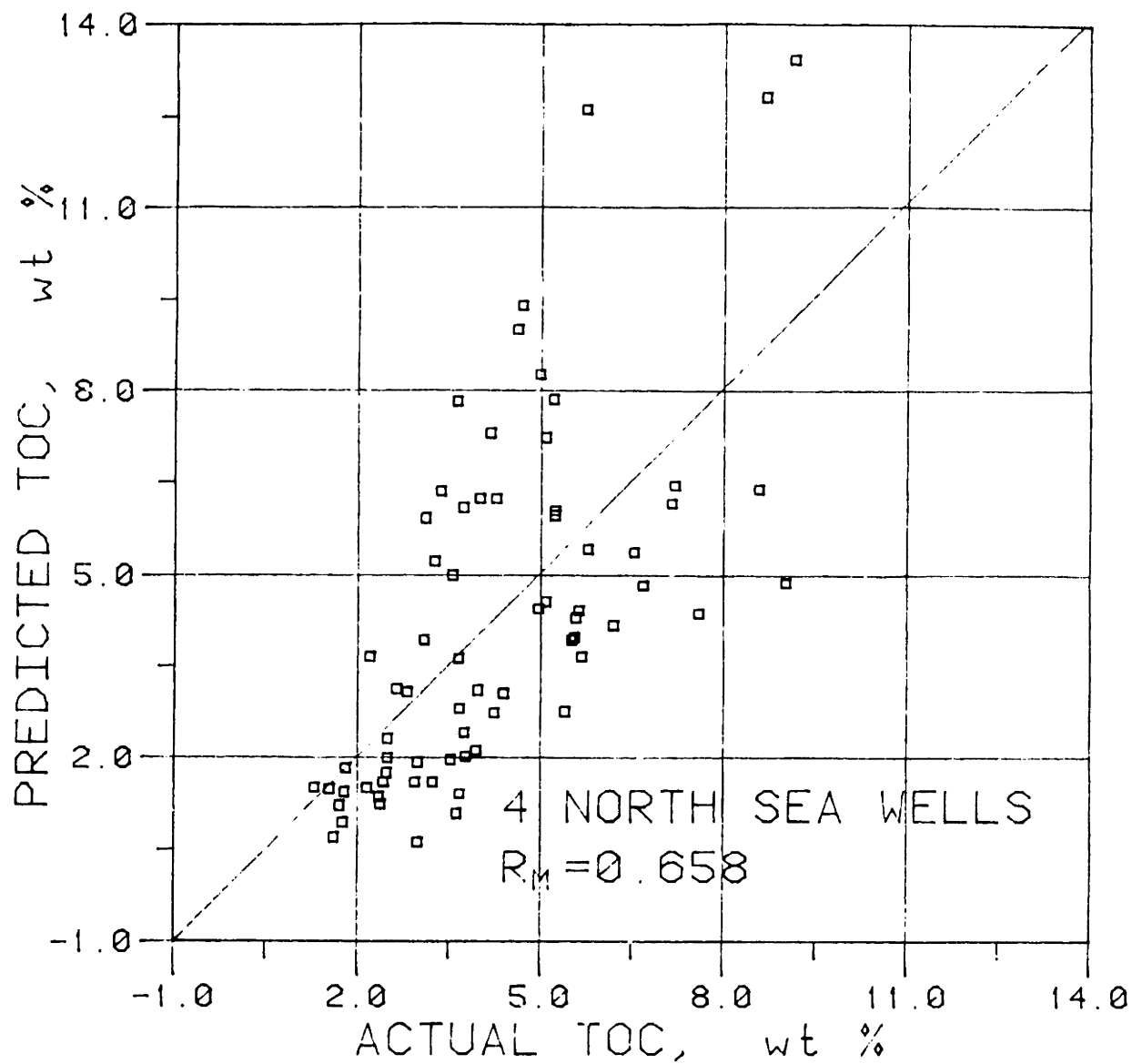


Figure 15E. Actual TOC versus TOC's obtained by regressing all of the North Sea Data simultaneously.

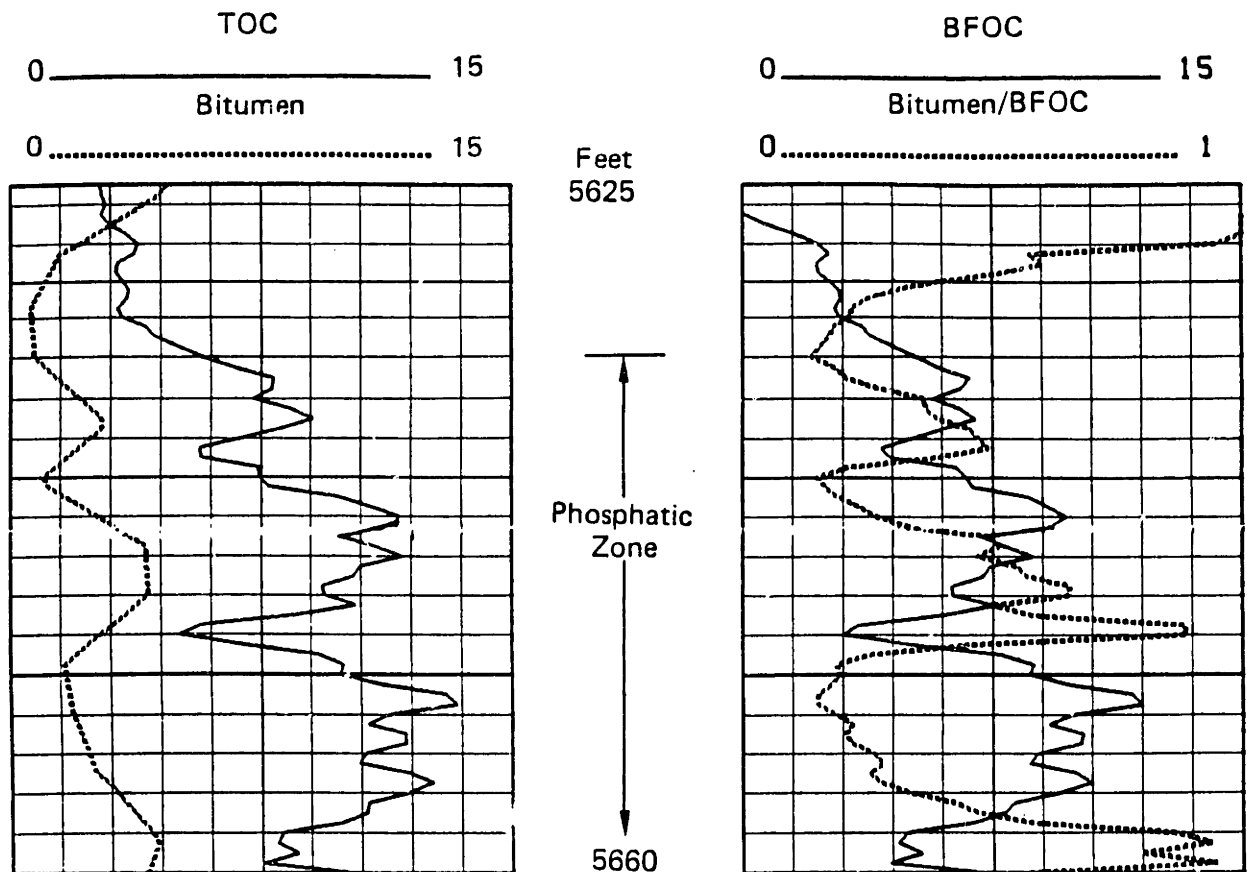


Figure 16. Geochemical data obtained from drill-core samples above and in the Phosphatic Member of the Monterey formation in the California well. Actual data (tabulated in Appendix F) have been smoothed to better approximate the spatial resolution of a logging device. Depth scale is 2 feet per division.

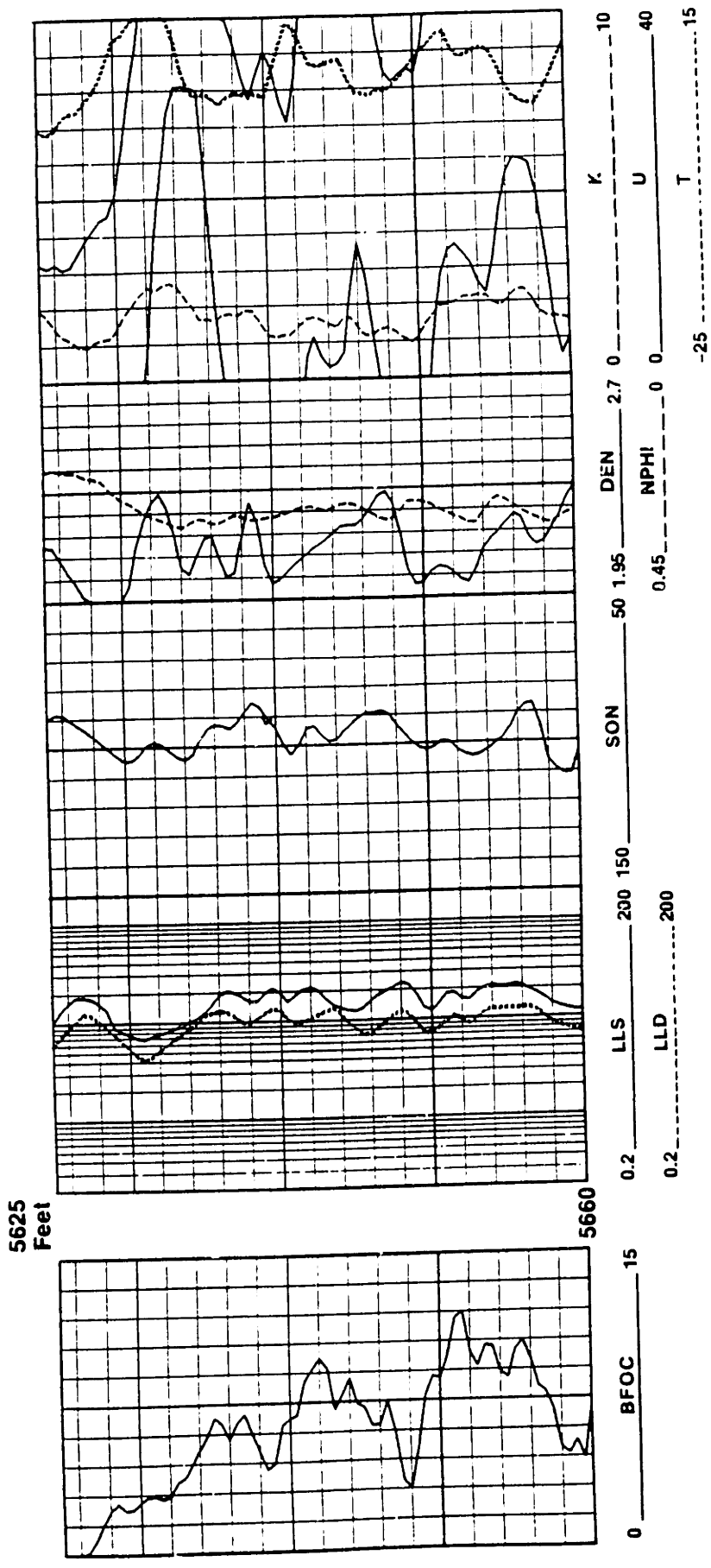


Figure 17. Geophysical logs available for source rock evaluation in the California well. Increasing BFOC indicates the top of the organic-rich phosphatic zone. For log nomenclature, see Appendix E.

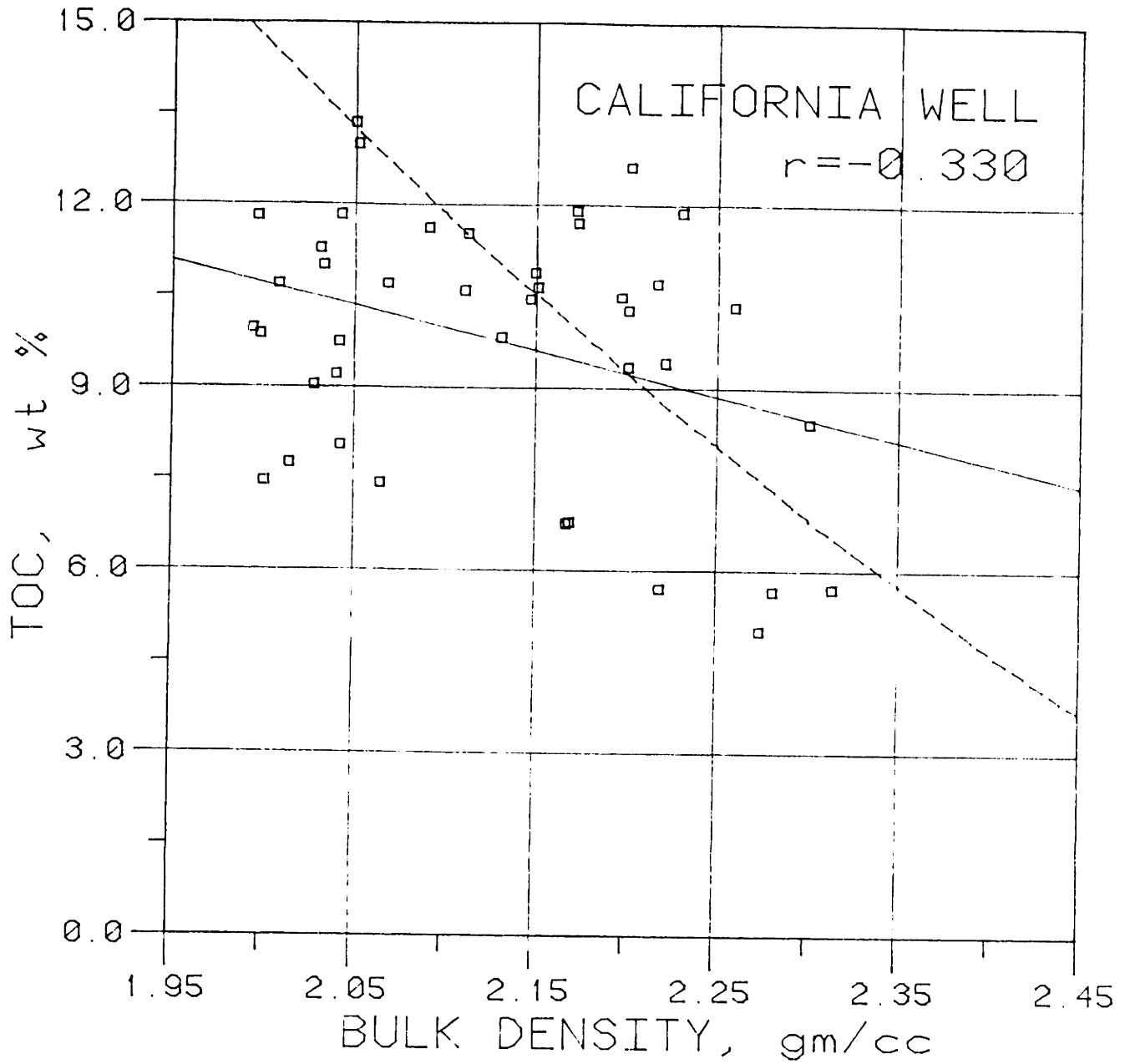


Figure 18. Plot of TOC versus apparent bulk density for the California well. Solid line is from least squares regression. Dashed line is the prediction by volumetric averaging with a matrix density of 2.65 grams/cc. Data to the left of the model line exhibits a low density phase which is unaccounted for in the model. Likewise data to the right of the model line probably contain the heavy minerals apatite and pyrite.



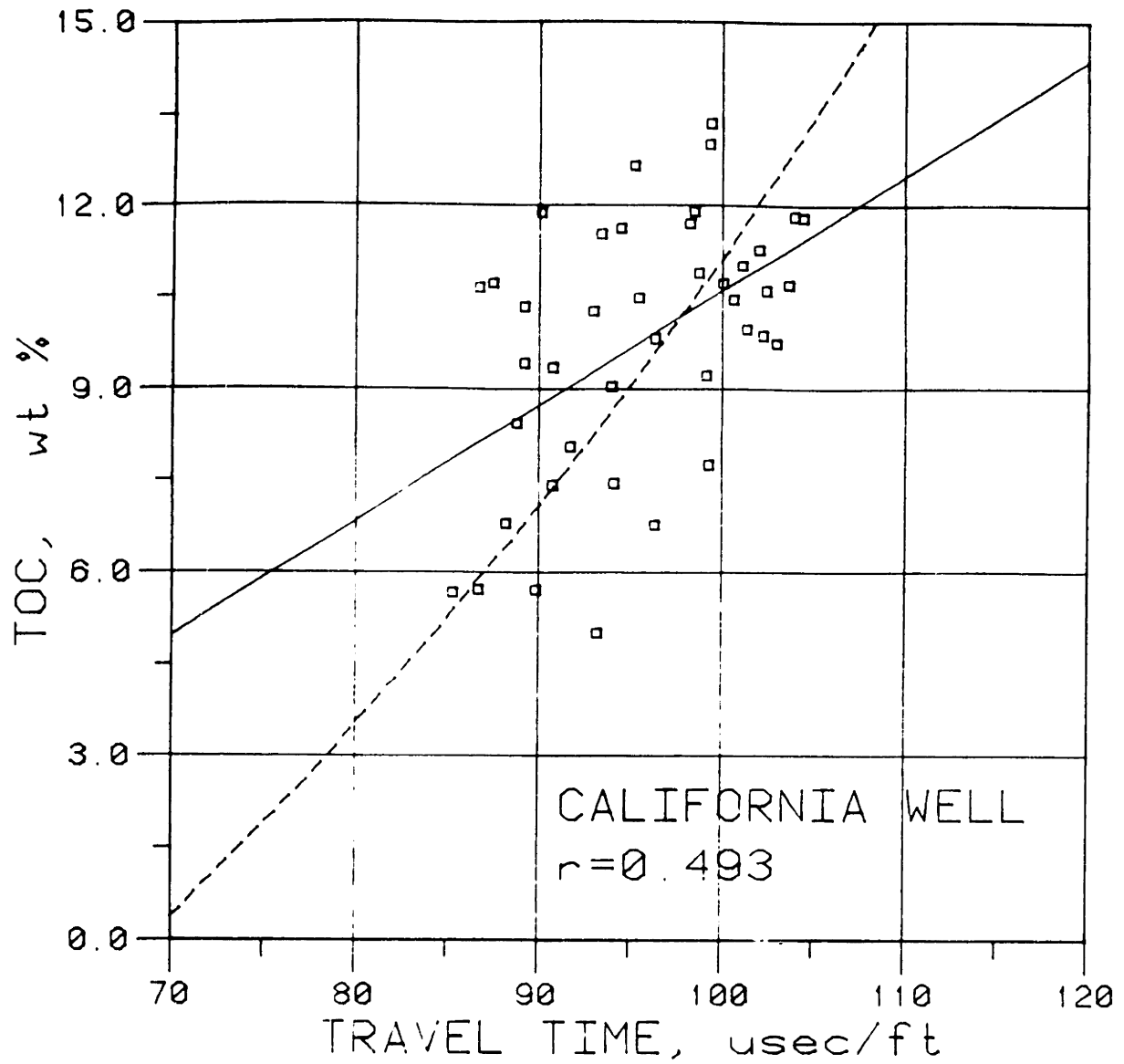


Figure 19. Plot of TOC versus sonic travel time for the California well. Solid line is from least squares regression, dashed line from volumetric modelling. Parameters used in modelling are listed in Table 14. Variability in travel times is unusually small considering the range of densities encountered. This could be a problem of limited tool resolution to thin beds.

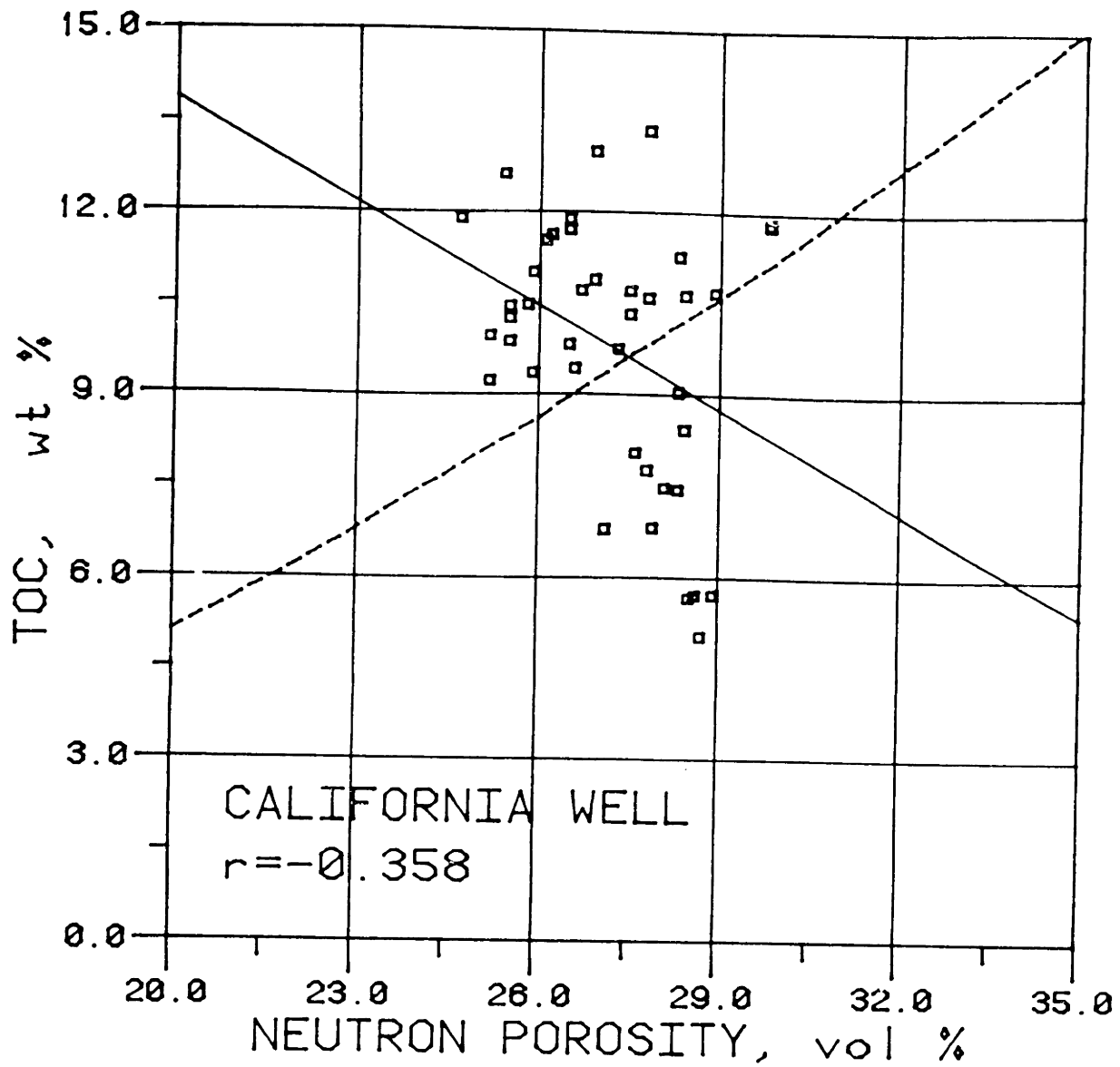


Figure 20. Plot of TOC versus apparent neutron porosity for the California well. Solid line is from least squares regression, dashed line from volumetric modelling. Parameters used to calculate the model response are listed in Table 14. Note the small range of neutron porosity values. The apparently negative correlation between neutron and TOC is not easily explained.

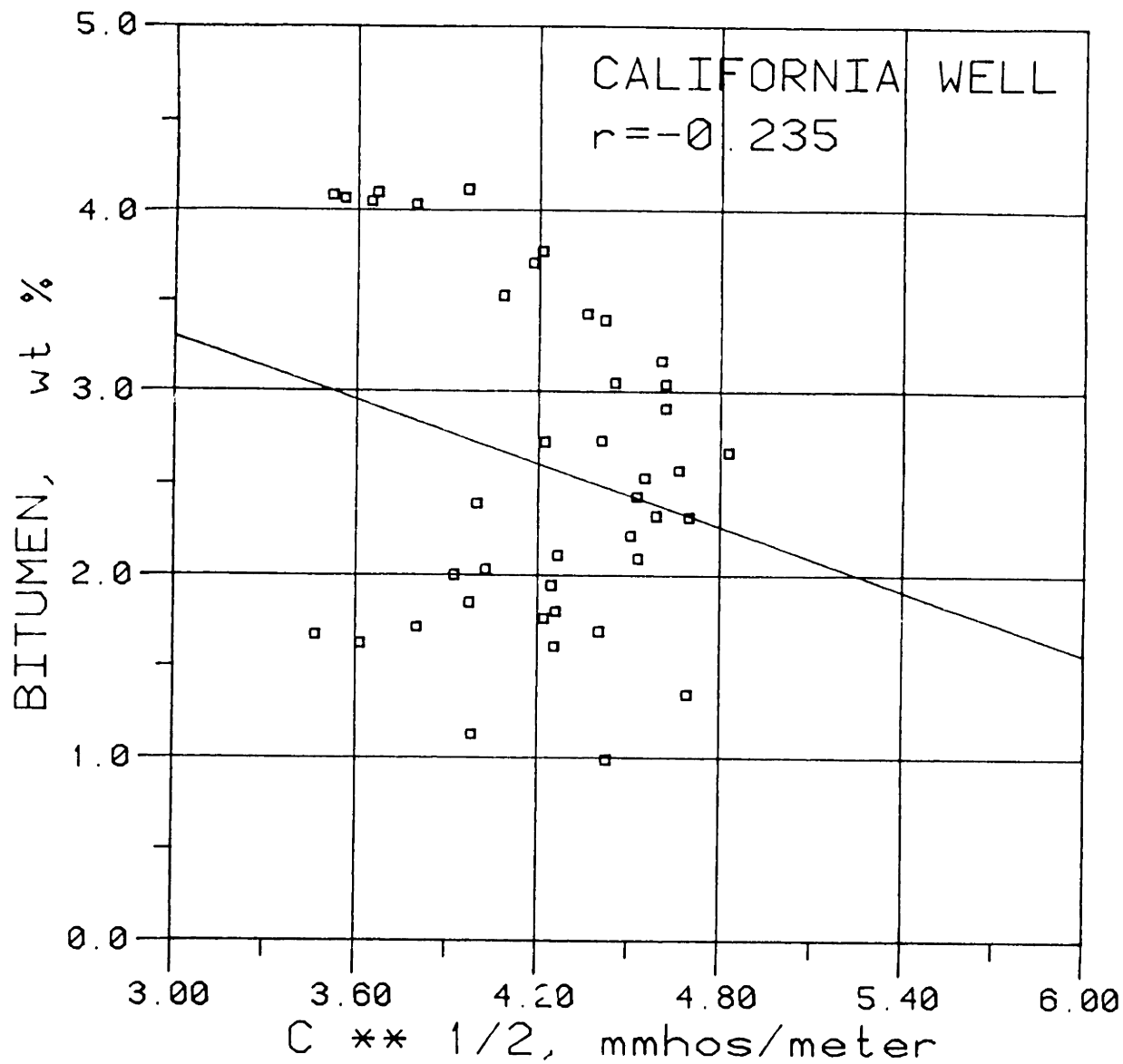


Figure 21. Crossplot of bitumen concentration versus the square root of conductivity. Although the correlation is not strong, this supports the hypothesis that the resistivity log may allow a qualitative assessment of maturity.

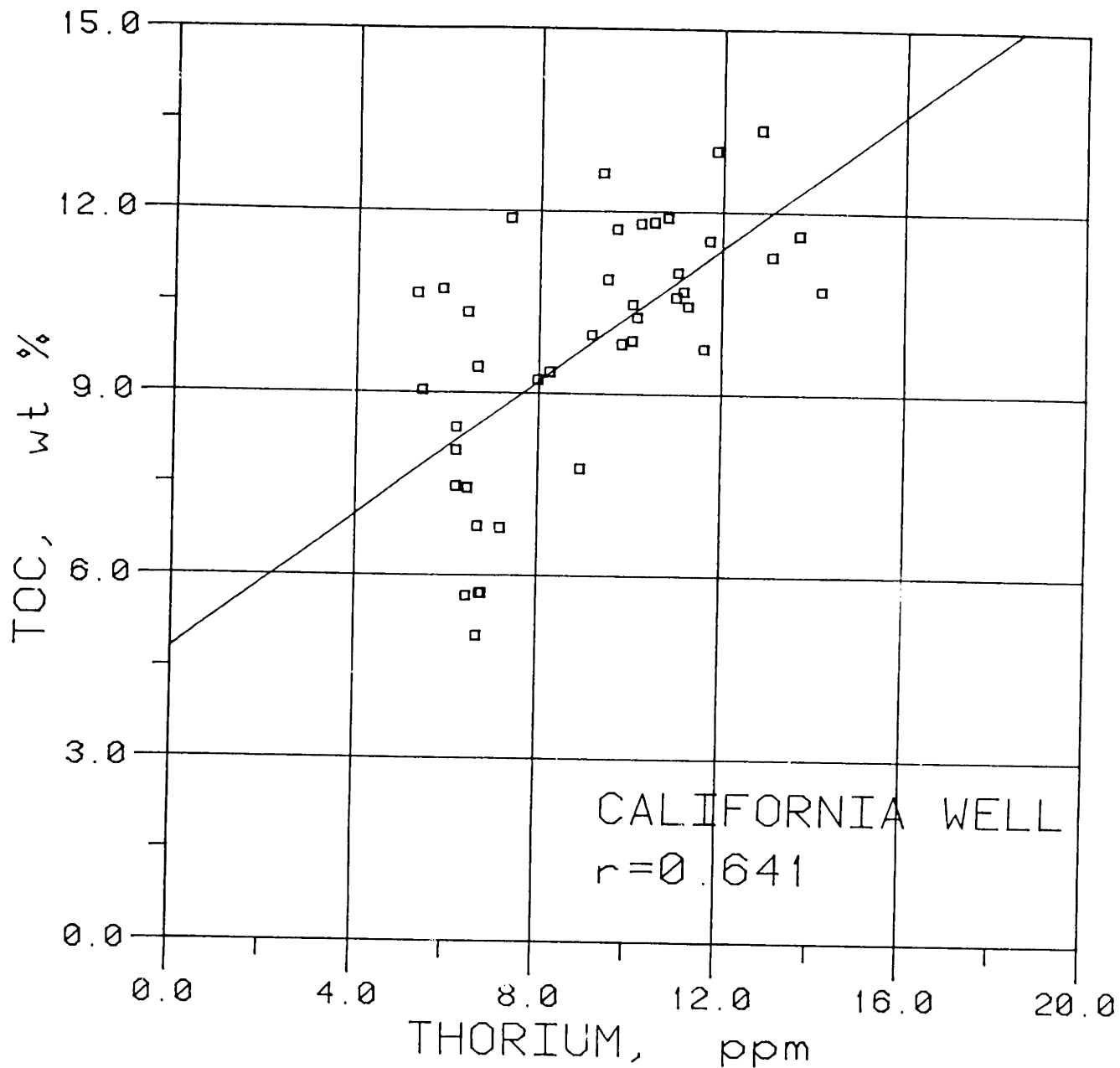


Figure 22. Plot of thorium abundance versus TOC for the California well. Clay content, of which thorium is often an indicator, is generally associated with increasing organic content.

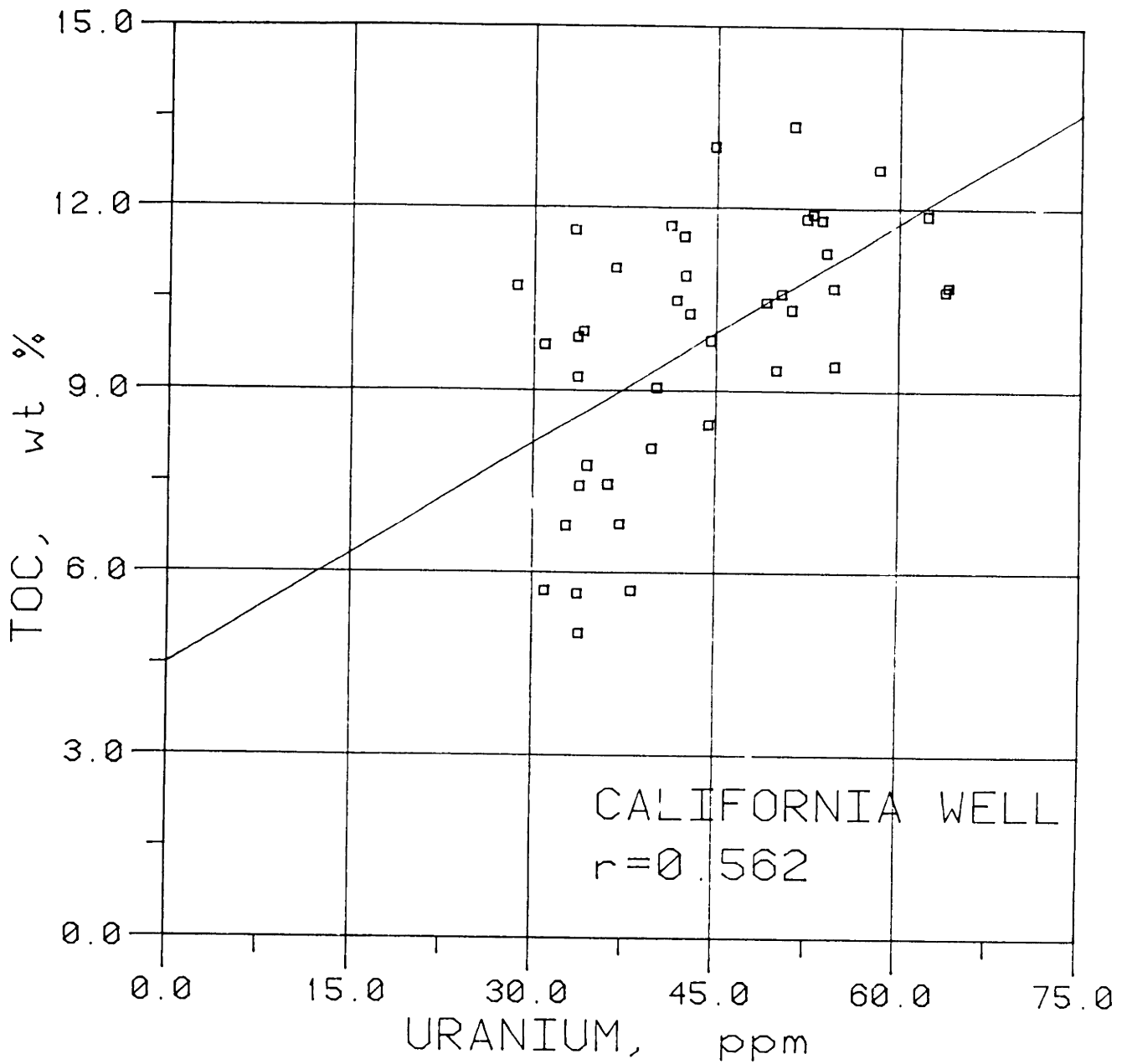


Figure 23. Plot of uranium abundance versus TOC for the California well. The lack of linear association may be due to insufficient vertical resolution in the logging sonde, and also to the association of uranium with phosphatic minerals.

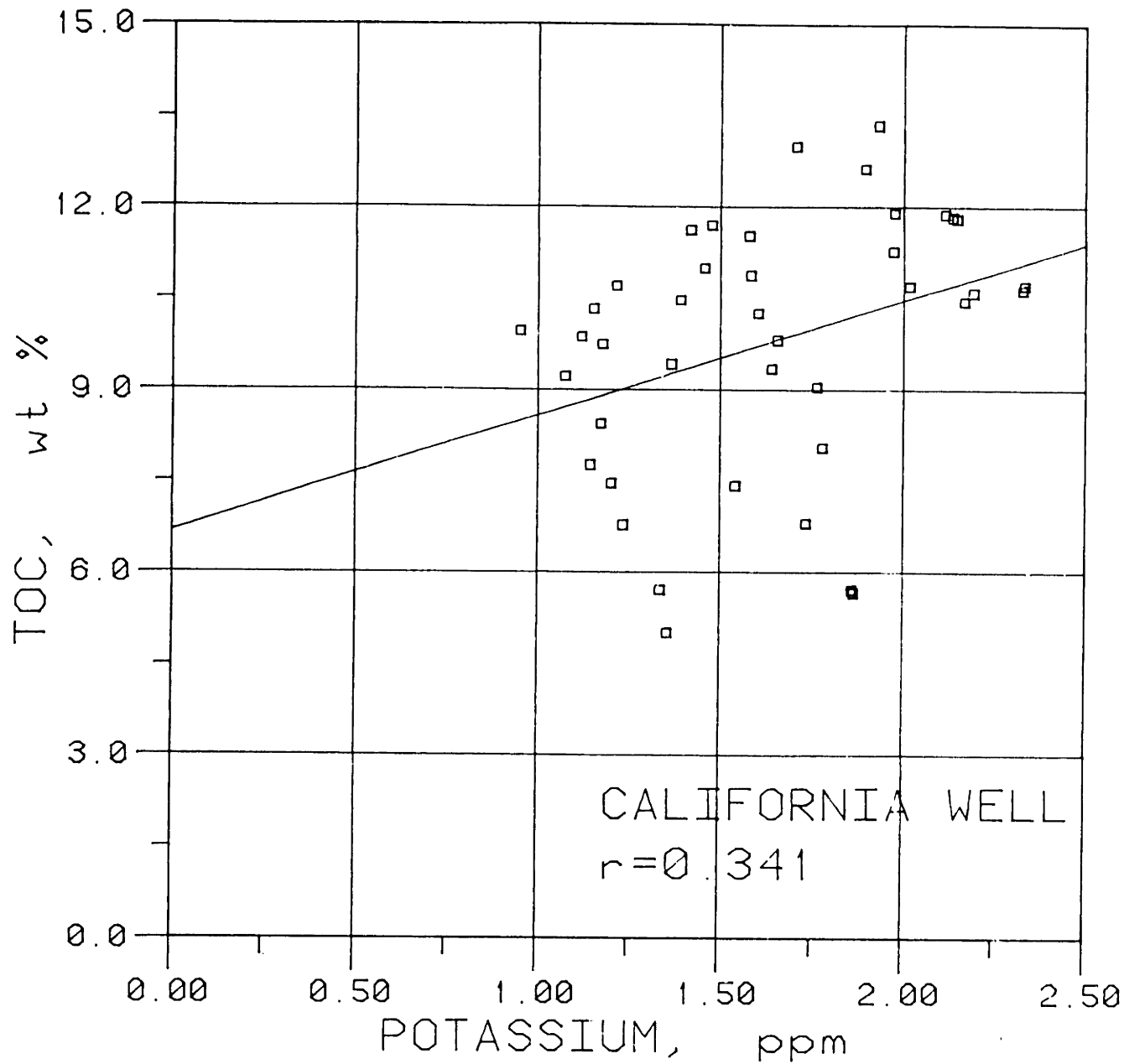


Figure 24. Plot of potassium abundance versus TOC for the California well.

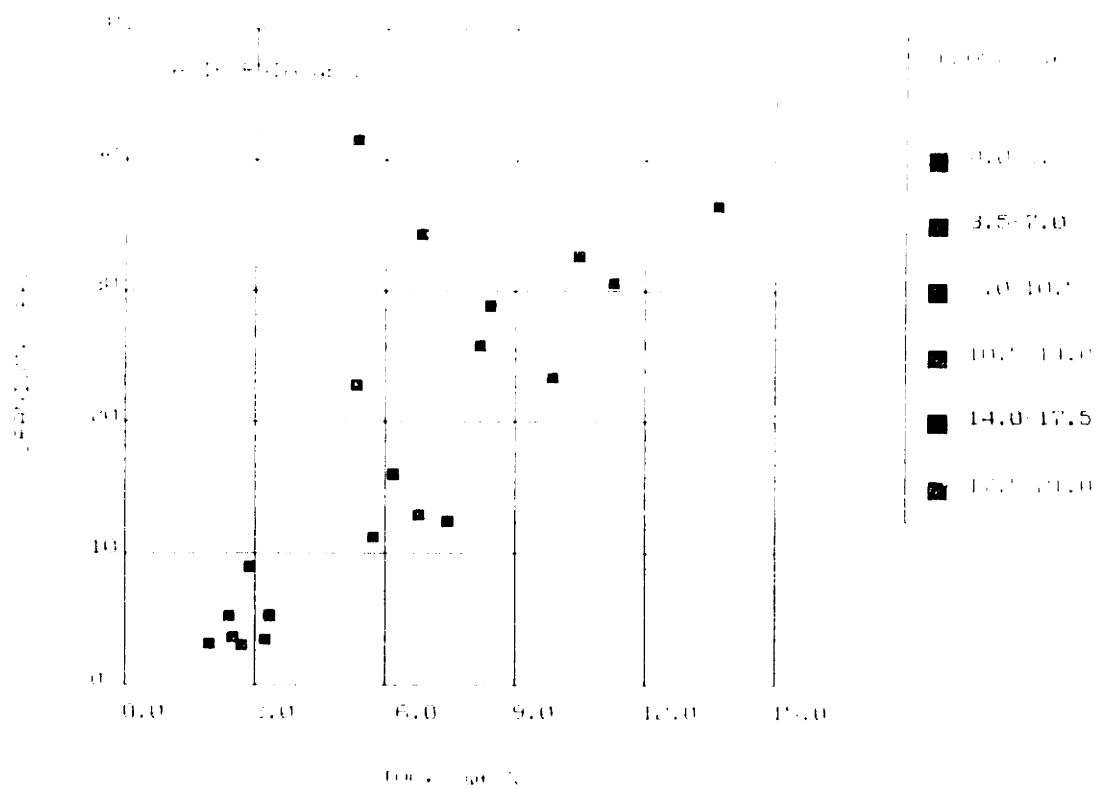


FIGURE 25. 3-DIMENSIONAL CROSS-PLAT DEMONSTRATES DEPENDENCE OF URANIUM ABUNDANCE ON CONCENTRATIONS OF TOC AND P205. REGRESSING TOC AND PHOSPHATE ON URANIUM CAN ELABORATE 91% OF THE URANIUM VARIABILITY.

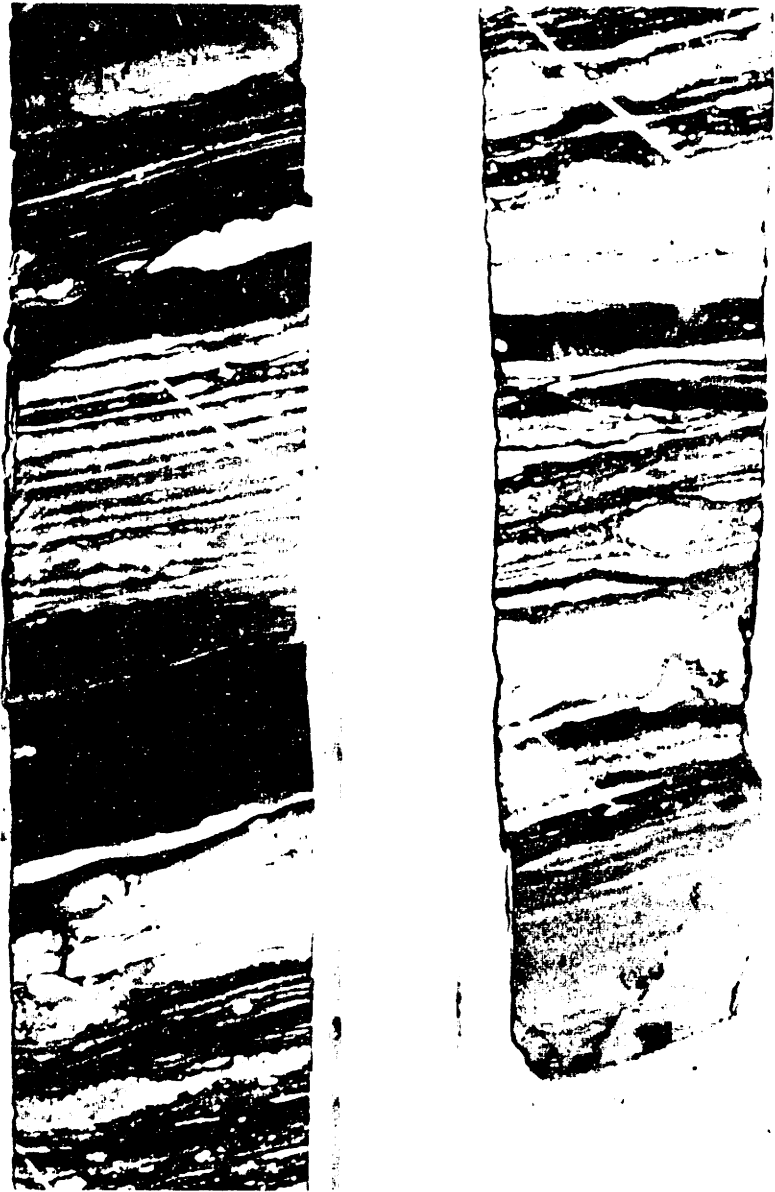


Figure 26. Black and white core photograph showing the complexities of a representative section of the phosphatic zone of the Monterey Formation. The darker phase is highly organic, and the lighter phase is highly phosphatic. Each core section is roughly one foot in length.



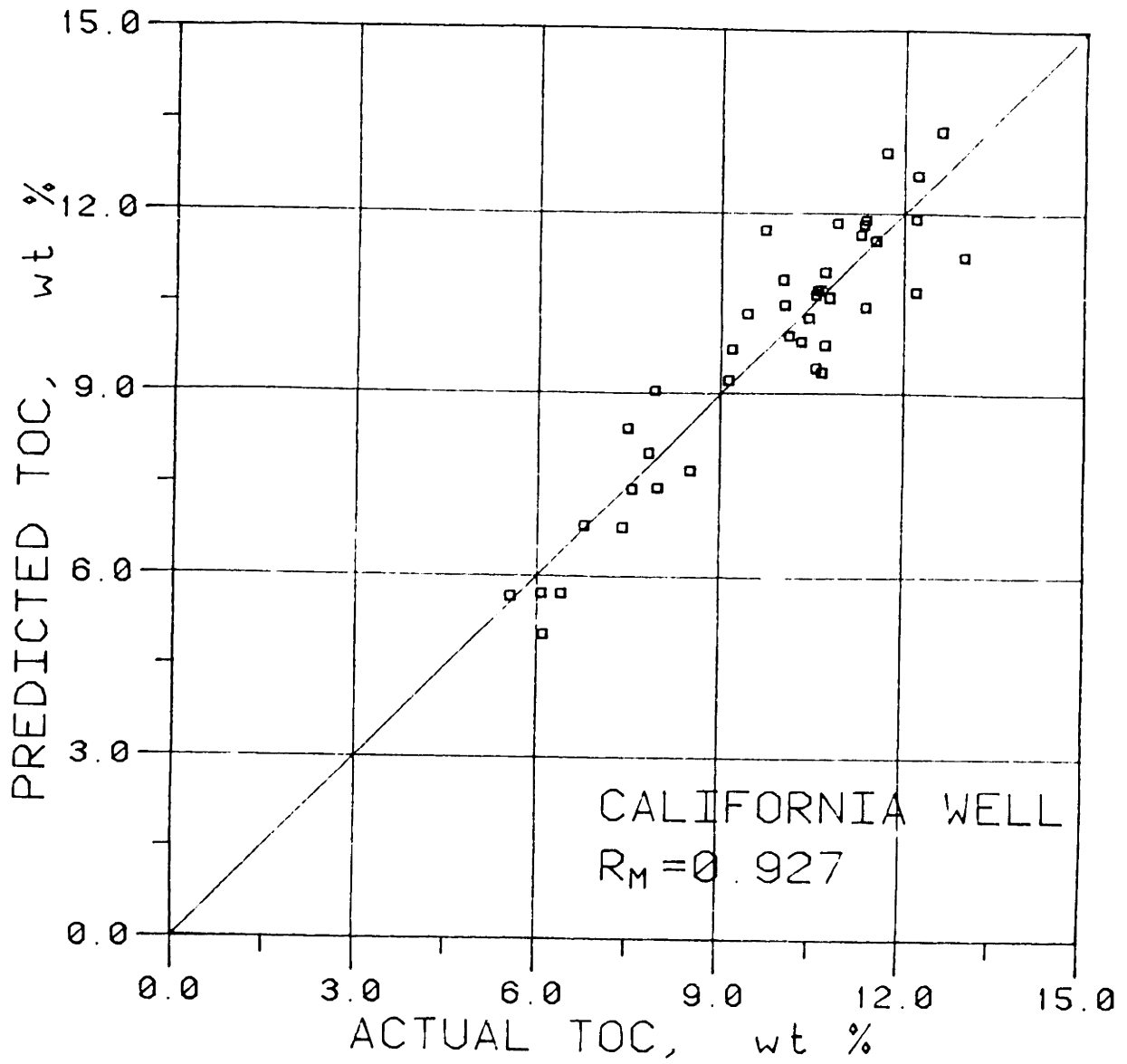


Figure 27. Predicted versus actual TOC's for the California Well, from multivariate regression (equation 12).